Creep behavior of Mg-Al-Ca based alloys

A thesis submitted in partial fulfillment of the

requirements for the degree of

Master of Technology

In

Metallurgical and Materials Engineering

By

B. Ravi Kiran Reddy

(Roll No: 212MM1334)

Department of Metallurgical and Materials Engineering
National Institute Of Technology, Rourkela
May 2014

Creep behavior of Mg-Al-Ca based alloys

A thesis submitted in partial fulfillment of the

requirements for the degree of

Master of Technology

In

Metallurgical and Materials Engineering

By

B. Ravi Kiran Reddy

Under the guidance of

Prof. Ashok Kumar Mondal

Department of Metallurgical and Materials Engineering
National Institute Of Technology, Rourkela
May 2014

CERTIFICATE

This is to certify that the thesis entitled, "**Creep behavior of Mg-Al-Ca alloys**" submitted by **B. Ravi Kiran Reddy** (212MM1334) in partial fulfillment of the requirements for the award of Master of Technology in Metallurgical and Materials Engineering at the National Institute of Technology, Rourkela is a bonafide research work carried out by him under my supervision and guidance.

To the best of my knowledge, the matter embodied in the thesis is based on candidate's own work, has not been submitted to any other university / institute for the award of any degree or diploma.

Date:

Supervisor

Prof. Ashok Kumar Mondal
Dept. of Metallurgical and Materials Engg.
National Institute of Technology, Rourkela
Odisha 769008.

ACKNOWLEDGEMENT

I take this opportunity to owe many thanks to the Department of Metallurgical and Materials Engineering, National Institute of Technology Rourkela for offering a unique platform to earn exposure and garner knowledge.

I wish to extend my sincere and heartfelt gratitude to my guide Prof. A. K. Mondal, a true guide who supported and encouraged me during the entire tenure of the project. He inspired me to drive this thesis towards the path of glory and success.

I also thank Prof. B. C. Ray, the HOD, Department of Metallurgical and Materials Engineering, National Institute of Technology Rourkela for granting me permission to do this project and avail all the facilities in the department. I also express my thanks to all other Professors of our department for their co-operation and valuable advice during the course work and my project work.

There are many who I may have left out in the acknowledgement, but whose co-operation no doubt went a long way in completing this project in time.

Date:

Place: Signature

(B. Ravi Kiran Reddy)

ABSTRACT

The role of intermetallic phases on the creep behavior of two Mg-Al-Ca based alloys MRI153M and MRI230D was investigated by characterizing the microstructures of both the alloys in as-cast as well as creep tested conditions. For comparison the AZ91 Mg alloy is also employed. The AZ91 alloy consists of $Mg_{17}Al_{12}$ phase, the MRI153M alloy consists of C36 ($(Mg,Al)_2Ca$) and $Mg_{17}Al_{12}$ phases, and the MRI230D alloy consists of C36 ($(Mg,Al)_2Ca$) phase. The creep tests were conducted at various temperatures using a stress level of 70MPa. The highest, medium and lowest creep resistance was exhibited by the MRI230D, MRI153M and AZ91 alloys, respectively. Microstructural characterization following creep tests revealed that the amount of $Mg_{17}Al_{12}$ phase was increased in case of AZ91 alloy, which deteriorates its creep resistance. In case of the MRI230D alloy the amount of C36 phase increased, which increased its creep resistance owing to the higher thermal stability of the C36 phase. In case of the MRI153M alloy the $Mg_{17}Al_{12}$ phase increased significantly. However, the volume fraction of C36 phase is less in it as compared to that of the MRI230D alloy and accordingly, the former alloy exhibited medium creep resistance.

The two Mg alloys MRI153M and MRII230D contains Ca which suppresses the above mentioned β phase and gives rise to new intermetallic phase C36 ($(Mg, Al)_2Ca$ along the grain boundaries and other Mg dendritic regions. The intermetallic C36 having higher melting point is effective to pin dislocations at superior temperatures and increases the creep resistance of the alloy. The precipitation of the above mentioned C36 phase will result in increase of steady state creep resistance in MRI230D. Hence it is observed that MRI230D has superior creep and mechanical properties than the remaining at the elevated temperature.

CONTENTS

ACKNOWLEDGEMENT		i
ABSTRACT		ii
CONTENTS		iii
LIST OF FIGURES		v
LIST OF TABLES		vi
Chapter 1.0	Introduction	01
2.0	Literature review	03
2.1	Introduction to Mg crystal structure	03
2.1.1	Magnesium in automobile sector	04
2.2	Magnesium slip systems	07
2.3	Super plasticity of magnesium	08
2.4	Magnesium applications	09
2.5	Magnesium alloy advantages	11
2.6	Magnesium alloy disadvantages	11
2.7	Effect of major and minor alloying additions	12

2.8	Designation of Mg alloys	13
2.8.1	Mg alloys containing Zr	14
2.8.2	Mg-Al alloys	16
2.8.3	Analysis of AZ91D Mg alloy	18
2.8.4	Mg-Al-Ca alloy system	19
2.9	Creep deformation mechanisms	22
2.10	Creep analysis and creep guiding mechanisms in Mg-Al-Ca alloys	26
Chapter 3.	Experimental procedure	28
Chapter 4.	Results and discussion	30
4.1	As cast microstructure	30
4.2	Creep behavior	38
4.3	Microstructural changes following creep	42
Chapter 5.	Conclusions	48
Chapter 6.	References	49

LIST OF FIGURES

Fig. 2.1	crystal structure of Mg and its crystal parameters	04
Fig. 2.2	Various planes and directions in HCP crystal	07
Fig. 2.3	Mg component used in fan housing	09
Fig. 2.4	phase diagram of Mg-Al system	16
Fig. 2.5	SEM micrographs of Mg alloy with 9% Al content	19
Fig. 2.6	Binary phase diagram of Mg-Ca system	21
Fig. 2.7	Standard creep specimen	23
Fig. 4.1	XRD pattern for AZ91D,MRI153M,MRI230D	31
Fig. 4.2	SEM micrograph of AZ91D Mg alloy	32
Fig. 4.3	EDS analysis of β phase ofAZ91D Mg alloy	32
Fig. 4.4	SEM micrograph of MRI153M Mg alloy	34
Fig. 4.5	EDS analysis of MRI153M Mg alloy	35
Fig. 4.6	SEM micrograph of MRI230D Mg alloy	37
Fig. 4.7	EDS analysis of MRI230D Mg alloy at C36 phase	37
Fig. 4.8	Strain vs. time plot for AZ91	39
Fig. 4.9	Calculation of strain rate from strain vs. time plot for AZ91	39
Fig. 4.10	Strain vs. time plot for MRI230D alloy	41

Fig. 4.11 Calculation of strain rate from strain vs. time plot for MRI230D alloy 41

Fig. 4.12 SEM micrographs of creep tested AZ91D alloy 43

Fig. 4.13 SEM micrographs of creep tested MRI153M alloy 45

Fig. 4.14 SEM micrographs of creep tested MRI230D alloy 46

LIST OF TABLES

Bond length of the alloying elements 04

Mechanical properties of AZ91D 06

Chemical composition of Mg alloys 29

Chapter 1. Introduction

1.1 Introduction

The light weight requirements in the automobile and transport sectors has become the crucial importance in the recent times. The large amount of energy consumption is done by the passenger vehicles which accounts to nearly 60% of total and is majorly responsible for the CO_2 emissions. This situation has arisen because to decrease the environmental emissions, to increase the efficiency and to meet the customer demands from day-to-day life. The power train components also requires a necessity of lightweight materials to fulfill the above mentioned requirements. Magnesium offers the various advantages when compared to the conventional metals like steel, iron. Mg is a lighter element which has lesser density when compared to Al, Fe and offers high specific strength, has better casting properties and good dimensional stability. Hence the research on the Mg in the light weight sector has been rapidly increasing in the recent times. The chief Mg alloys used in the automobile industry contains either Aluminum or rare earth alloy addition. Al alloy addition offers various advantages such as to improve the corrosion resistance, better cast ability, strength and creep resistance of the alloy. Generally power train components has to withstand the temperature of 150°C-200°C and the stress range of 50-70Mpa. But one of the major limitation with the Al alloy addition is the formation of the intermetallic β-$Mg_{17}Al_{12}$ phase which is having the low melting point along the grain boundaries. As the temperature increases, it softens and coarsens rapidly and decreases the creep resistance of the

alloy. Hence the Al alloy addition is only suitable for mediocre temperature range, but not for the higher temperature range. Hence β phase is responsible for the degradation of the creep properties in Mg-Al alloy systems. So the usage of the Mg-Al binary systems in the automobile industry is very limited.

In order to extend the range of applications, many research has been done on the Mg alloy with rare earth element (RE) alloy addition. It is found that with the small addition of RE, there is a rapid increase in the creep resistance of the alloys. But due to the high cost of rare earth, its usage has been limited. So the research have shifted to the low cost alloying additions such as Ca, Sn and Si. The above mentioned alloy additions will form the stable intermetallic unlike the β phase in the Mg-Al systems. Addition of surface active elements such as Ca in Mg-Al systems will suppress the β phase formation by forming the C36 ($(Mg, Al)_2Ca$) intermetallic which is having high melting point and is responsible for the increment of creep resistance. Ca is also responsible for the grain refinement which results in the finer grain size and results in the better room temperature mechanical properties.

1.2 Objective of the present work

In the present investigation, various creep tests are carried out on the Mg-Al-Ca alloys i.e. MRI153M and MRI230D under similar test conditions and they are being compared with the conventional AZ91D Mg alloy. Creep plots are plotted from the creep tests and their respective creep rates are being compared for the primal alloy addition at elevated temperature. A detailed microstructural analysis is being carried out before and after creep tests.

Chapter 2. Literature review

2.1 Introduction to Magnesium crystal structure

Magnesium was first invented by British chemist Sir Humphrey Davy in 1808 from its Magnesium sulphate during an electrolytic process [1]. Magnesium is the sixth most abundant element on earth. The development of Mg has grown rapidly during world war. Mg generally forms the hydroxide film known as Magnesium hydroxide if it is left in the atmosphere [2]. Considering the crystal structure, Mg generally has hexagonal crystal structure having the crystal parameters as a = 0.3209 nm and c = 0.5211 nm with c/a ratio of 1.624. The lattice parameter of the magnesium unit cell (a=0.3209 nm) is such that it allows the addition of a wide range of solute elements, such as aluminum (Al), zinc (Zn), manganese (Mn), zirconium (Zr), strontium (Sr), calcium (Ca), etc., which can be found in commercial magnesium alloys. As the temperature increases rapidly, we observe an increment in the crystal parameters in the Mg, at the temperature of 597°C the values of a and c are 0.00573 nm and 0.00962 nm respectively, with c/a ratio as 1.62458 [1]. During the alloying addition of Mg there is an increment in the lattice parameters have been observed. If we consider the Mg-Ca binary alloy system, the lattice parameters for the pure Mg are increased to a = 0.32125 nm and c = 0.52656 nm with c/a ratio as 1.6391 [3]. This can be explained because the Ca has larger bond length when compared to that of the Mg. various alloying elements with their corresponding bond length is shown in table. 2.1. From the table it can be seen that all the alloying elements have higher bond length when compared to that Mg. Thus the Mg binary additions will increase the lattice parameters of Mg.

Mg	Al	Ca	Sr	Ce	La
320	286	394	430	365	374

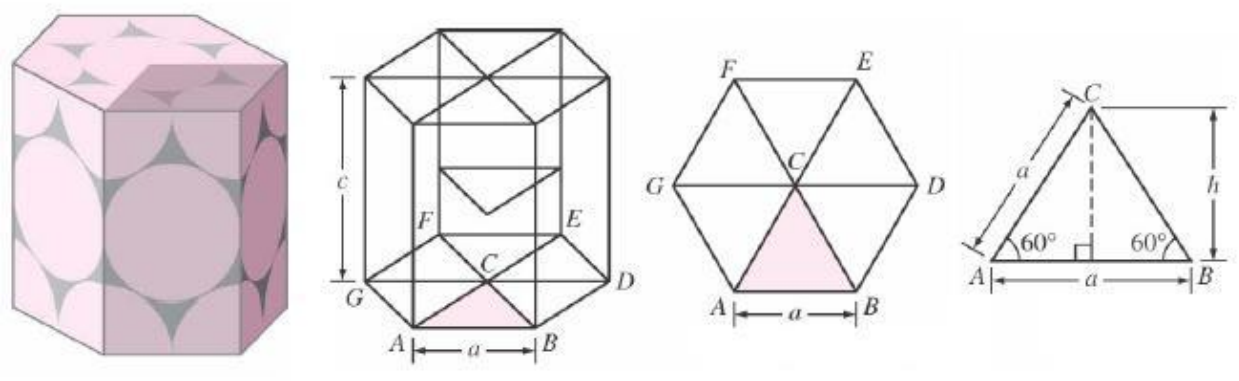

Fig. 2.1 shows the crystal structure of Mg and its crystal parameters

2.1.1 Magnesium in automobile sector

The modern luxurious trend and the developments in the safety features of contemporary automobile have witnessed an increase in vehicle weight, contributing its amount to the fuel consumption and the CO_2 emission. An average increase in weight of over 20% in the two decades is evident in the automobile industry [4]. Most of the increased weight constituents increased the engine size along with the addition of safety features, especially with the use of steel. In the last two decades, significant increases in the use of light metals such as titanium, aluminum and magnesium alloys are evident. Furthermore, the consumption rates of these materials are continually increasing because of the ever increasing pressures for higher performance and fuel economies. Hence, the importance of weight reduction posed a crucial and

a challenge for automobile producers that led to improvement in the fuel economy, in addition to reducing the green house effects and other environmental issues [5]. It is necessary to reduce the vehicle weight and by the replacement of steel by light metal alloys, it is near to possible. The low strength room temperature applications move towards the plastic and polymer composites, especially in the frames and interior body covering of all passenger cars [6]. However, most of the engine components made from ferrous material are now being replaced by aluminum and magnesium alloys [7]. The major aim of the researchers is to find suitable material that is more efficient than Al so as to reduce the weight of automobiles still further. Mg and its alloys are one such promising material whose lightweight advantage could be used for the above said purpose. The first Mg that is produced commercially was in Germany in 1916 [8]. However during the initial stages, the total global production of Mg is a paltry of 300 tones [9]. But during the World War II, its production has been rapidly increased. The demand for Mg has been increasing rapidly with an annual growth of 7.2% annually until 2012 as it is the light structural element and has a wide range of applications in the transportation sector. Magnesium generally has very low density which is 1.74g/cm^3, when compared to that of the conventional metals like Aluminum, iron, and steel. It also offers various advantages in various other fields such as high specific weight, machinability, good cast ability and excellent damping characteristics. Now a days Magnesium are generally utilized in room temperature applications in automobiles such as body frames, body panels, and seat valves. High pressure die casting (HPDC) is generally the most common technique that has been widely used for the mass production and high efficiency. HPDC will result in the finer grain size which incline to better mechanical properties at the room temperature. However the HPDC parts may suffer from various casting defects chemical segregations and porosity bands which will generally observe

in the surface parallel to casting. Several researches has been done to increase the grain refinement of Mg by either physical or chemical routes. Chemical route involves the alloying addition to the Mg which will result in the better grain refinement. Many researchers are trying to increase the efficiency of the automobiles by implementing the Magnesium in high temperature applications where the

Temperature range is generally 150°C-200°C. However as the temperature increases, Mg faces the reduction in strength. Among various Mg binary alloying additions, Mg-Al system has been mostly used because Al has better cast ability. Below are the various mechanical and physical properties of the conventionally used Mg alloy AZ91D.

Properties	Magnesium AZ91D alloy
Yield strength (MPa)	160
Tensile strength (MPa)	230
Elongation (%)	$0.5*10^{-3}$
Shear strength (MPa)	140
Elastic modulus (GPa)	45
Density (g/cc)	1.81
Specific heat (J/Kg/°K)	1050
Expansion Co. eff .($x10^{-4}$/°K)	26
Thermal Conductivity (W/M°K)	72

2.2 Magnesium slip systems

Several researches have been done to find out the number of active slip systems in Mg alloys. The various slip systems in the Mg are basal, prismatic, first order pyramidal and second order pyramidal i.e. {0001}, {101¯0}, {101 ¯1}, {112 ¯2}. Table 2.3 shows the various slip planes and slip directions. Among all the slip planes in the Mg, basal slip plane is more favorable as the other slip planes depends on the various other factors like temperature, amount of the alloy composition. A research indicate that at the room temperature, for pure Mg the critical resolve shear stress should be around 0.45 Mpa for the slip whereas under the same conditions the stress should be around 0.50 Mpa for the first order pyramidal plane . So the above data indicate that slip will primarily occur in the basal plane then it moves on towards the first order pyramidal. Plastic deformation of the magnesium crystal occurs by slip in the <1 1 2 ¯ 0> directions on the basal planes and by twinning on the pyramidal {1 0 1 ¯ 2} planes at temperatures below 498K. However, deformation is easier when the temperature is increased above 498K, as additional pyramidal {1 0 1 1} slip planes become operative. This explains why magnesium alloys have limited cold formability but are readily hot worked

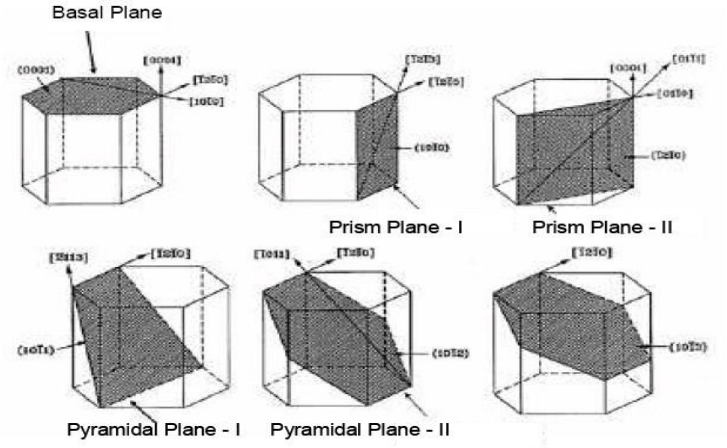

Fig. 2.2. Various planes and directions that are observed in HCP crystal

2.3 Super plasticity of Magnesium

Super plasticity is defined as the property of the poly crystalline substance that exhibits huge elongations while subjected to the tension in the material which is generally above 190% before the failure occurs. The value n which shows in the below equation is known as strain rate sensitivity is generally the measurement index for the super plasticity of the materials. It is generally high for the super plastic materials when they are subjected to the tensile deformation [10]:

$$\sigma = A\ \acute{\varepsilon}^{n}$$

In the above equation σ is known as the true flow stress, ἑ is known as the strain rate, A is generally the constant and its value is generally 0.22 for most of the metals and the alloys generally exhibit n value less than 0.22.where as in the case of super plastic materials it is generally higher, usually in the order of 0.35. For most of the metals this Super plasticity is generally occurs at the high temperature, it is generally 0.45-0.55 times its melting point .

2.4 Magnesium applications

2.4.1 Aerospace applications

Magnesium and its alloys are extensively used in the aerospace industries for the manufacture of the aircraft wheels, body frames, and airliner engines [11]. Magnesium is generally used in the airlines because for the aircrafts the prior factor is light weight without compromising on the strength. Magnesium and its alloys generally has the high specific strength, less weight and high machinability. Mg alloys should sustain the high stress and superior temperatures. Most commonly used Mg alloys for air liners are WE43, QE22, ZE41 which are basically the Mg and

rare earth alloy additions due to their superior properties at prior temperatures and also their corrosion resistance capability.

Fig. 2.3. Shows the Mg component used in fan housing

2.4.2 Military applications

Mg and its alloys are generally used in military and the defense sectors. This is due to the fact that the Mg alloys have high rigidity and less weight without compromising on its strength and the alloys also are easily machined. Mg alloys are generally used for the rocket launchers and missile bodies and satellite interiors. The generally used Mg alloys are ZE41 and EZ33 and also ZK51 which are mainly Mg-Zn-Zr alloys are used in the satellites and missiles manufacturing [12].

2.4.3 Automobiles sector

Mg alloys are chiefly and majorly used in this sector as the light weight vehicles are generally preferred due to their better efficiency and less fuel intake and also due to global concern. Researchers are focused on the new Mg alloying elements to increase the Mg alloy usage in the automobile sector. AZ91D is the chiefly used Mg alloy in the transportation sector, but the main disadvantage is its less creep resistance at the higher temperatures. The various that are being manufactured by the automobile industry is seat frames, engine blocks, body frames, cylinder heads and its covers, oil pumping, lubrication housing and its pipe line. But vast research has to be done in the usage of the Mg alloys by alloying it with various elements in order to sustain the elevated temperatures and the improvement of corrosion and creep resistance of the alloys [13].

2.4.4 Atomic and nuclear powered applications

In the nuclear reactor with the uranium as the chief component, the ejected neutrons are very much essential and it is very much important to preserve the neutrons from being. The nuclear power plants generally releases the large amount of the energy and will have high temperature at its core. For the better power production from the nuclear power plant it is generally necessary for the plant to have the better design layout and the proper choosing of the canning material. Mg is the better choice of the canning material among all and in order to increase the efficiency furthermore it is recommended to use magnesium dioxide as the coolant gas [12]. Mg alloys are generally used because it has superior conductivity, it has low efficiency towards neutrons absorption, it has high carbon resistance and the important one is it cannot be possible of alloying Mg with uranium. [12].

2.4.5 Electrical and athletic equipment's

Pure Mg and its alloys also finds a variety of applications in electrical and also gaming sectors. Mg alloys are generally used in the computer manufacturing and telecommunication sectors. Mg alloys are generally used because of its shielding towards electro magnetism and the slender casings. Various fitness equipment and luxury sports cars are also made by Mg

2.5 Mg alloy advantages

As the various applications above mentioned with the Mg alloys are due to some peculiar characteristics of the Mg when compared to the other Metals or alloys. Transportation sector is largely benefited by the Mg and its alloys because of its higher efficiency and better fuel capability and the Mg alloys usage has been expanded rapidly. Mg alloys offers a large benefits such as high specific strength, better machinability, high shielding towards electro magnetism and better dissipating heat capacity, good casting properties and better damping capability [13].

2.6 Mg alloys disadvantages

Mg alloys are also being suffered with various disadvantages which limits usage in the various fields. Due to this constraints various research is carrying on the Mg to increase its properties and usage, but still Mg usage is still challenging in various fields. Various constraints that are facing by the Mg are Mg alloys are very costly when compared to conventional metals, there is a less possibility of recycling in the Mg, strength and various mechanical properties are relatively poor in elevated temperatures, the supply of Mg is very limited and Mg alloys are also facing poor corrosion and creep properties at the prior temperatures which limits their usage in transportation field.

2.7 Effect of major and minor alloying additions

2.7.1 Aluminum

Aluminum is the most commonly and chiefly used for alloying in Mg. The major factors responsible for this is because Al will enhance casting ability and also Al is easily soluble as the solubility is as high as 12.73% in the pure Mg at the temperature of 439°C [14]. With the addition of Al in Mg it forms the low melting point intermetallic $Mg_{17}Al_{12}$ along the grain boundaries. This newly formed intermetallic will induce the hardness to the alloy at the low temperature applications. Other advantageous factors upon the addition of Al is, the ultimate tensile strength increases very rapidly and reaches maximum and then it decreases. The same trend is followed by the ductility, but the decrement is very steep [15]. The Al solubility increases with increase in temperature and reaches the optimal value and decreases. At room temperature it value is around 1.9%. But one of the major disadvantage with Al is it enhances the porosity and therefore helps in the depletion of the properties [16]. However alloying the Al in Mg alloys are also economical, as it is cheap, and it also helps to enhance the resistance towards corrosion.

2.7.2 Zinc

Zinc, like Al is also highly soluble in the Mg. Zinc is the main factor which determines the nature of the intermetallic during the solidification. The amount of Zinc describes the nature as lamellar or divorced. By the addition of zinc, it helps to enhance the strength in the alloy by strengthening of solid solution. One of the other beneficial factor is, it has high flow ability which helps for manufacturing of intricate shapes. But the major limitation related to it is, the formation of

cracking when there is an excess amount of Zn. It also responsible for the decrement in the ductility of the alloy and helps to enhance the porosity in the alloy [17].

2.7.3 Manganese

The benefit by alloying Mn with Mg is that it enhances the resistance towards corrosion .when Mn is added to Mg it forms the new intermetallic which is Al-Mn-Fe based in nature [18]. Due to high density this intermetallic particles precipitate towards the melt bottom. In this way the Fe impurities in the alloy can be rectified. It also helps to reduce the efficiency of the remaining Fe particles by making them as cathodes with relative to the intermetallic formed which is of Al-Fe based in nature.

2.8 Designation of the Mg alloys

Mg alloys follow a particular code which has been adopted by the American Society for Testing Materials (ASTM) and this code is being used globally all over the world. This code generally contain two alphabetical letters which is trailed by the numbers besides them. This numbers generally represent the various compositions of the important/chief alloying elements. The various alloying elements that are chiefly used in the Mg are rare earth metals designated by E, Zirconium designated by K, Aluminum designated by A, Manganese designated by M, thorium designated by H, zinc designated by Z, Lithium designated by L.

Among the two alphabetical letters, first alphabetical letter designates the chief/major alloying element and the second alphabetical letter designates the minor alloying additions in the weight percentage. Mg alloys are generally been divided into two major groups one is the alloys which

are containing Zr whereas the second one represents the alloys which do not contains Zr. As the Zr alloying addition in the Mg is better responsible for refining of the grains in Mg and is beneficial for the room temperature properties. But, if the Al is the main alloying element in Mg alloy it will suppress the Zr as it forms the new intermetallic (Al-Zr based)

2.8.1 Mg alloys containing Zr

The binary alloying system of Mg-Zr has some constraints in its applications, hence its usage has been limited industrially. The Zr that is soluble in Mg which is in molten state is as high as 0.58%. But the most advantageous factor is that by alloying the Zr with Mg, there is high extent of grain refinement. For example in ZKSI (Mg-4.5Zn-0.7Zr) alloys consists of Zr that is being added to the Mg-Zn system in order to improve the grain refinement and to improve its mechanical properties. But there are restraints to these type of the alloys in industrial applications, as these alloys are subjected to the porosity and welding is very difficult which limits their usage. [19]. The other alternative to strengthen the alloys at the higher temperature is by the addition of the rare earth (RE) elements with Zn containing alloys.

Rare earth alloying additions are favored because the smaller addition of the RE will increase the creep and corrosion resistance of alloy to the vast extent and also various solid solutions are formed with Mg by alloying various RE elements. But the major disadvantage regarding the RE alloying addition is the cost of the alloying elements which is not economical. Hence by the alloying addition of all the three above mentioned elements like Zr, Zn, RE are all present in alloy then it will exhibit superior mechanical properties at the elevated temperatures. In the above mentioned alloy, Zr is used for grain size refinement and RE is used to improve creep and

corrosion resistance. For example EZ33 (Mg-3RE-2.5Zn-0.6Zr) has all the three elements and can be able to withstand the temperature 260°C [20].

Now a days a variety of researches has been done on the yttrium alloy addition, this is due to the fact that yttrium has greater solubility in Mg. A variety of Mg-Y-Zr combination alloys are commercially produced as they can withstand and preserve the strength at the elevated temperatures of about 300°C [21]. The preferable alloy of the above combination that is available commercially is WE54 as it contains yttrium 6 wt.% and also Nd of 2 wt.% which gives prior strength and suitable ductility.

Thorium alloying addition with Mg-Zr binary system is also chiefly used as it increases the strength and decreases the creep deformation and this alloy can be used at the temperature as high as 350°C. For example consider HK3l (Mg-3Th-0.7Zr) alloy contains ternary system and is generally used for the manufacturing of airliners and rockets. But the major limitation with the above alloy it is dangerous to the environment and hence its applications are limited. Another way to increase the mechanical properties of Mg alloy is by alloying it with silver (Ag). Hence the combination of Mg-RE-Ag-Zr system will possess the superior properties at prior temperatures [22]. Another Mg alloy that finds a variety of the applications in recent times are QE22 (Mg-2.5Ag-ZRE-0.7Zr) which is used in airliner frames, transmission housings, aircraft wheels

2.8.2 Mg-Al alloys (Zr free)

Al is the chief component that is being alloyed, in most of the Mg alloys. But most of the Mg – Al binary systems offers various limitations as they have poor creep resistance and their applications are limited. The chiefly used Mg-Al alloy is AZ91D, AM50 [19]. One of the major advantage with Al is it provides the better cast ability and has high strength and various mechanical properties.

But one of the major limitations regarding Mg-Al alloying system is that it cannot withstand elevated temperatures (>150°C) [23]. So other alloying elements are added in order to increase the properties at the superior temperatures. Si is added to this binary system which can increase the creep resistance of the alloys which is superior to that of the AZ91D. Alloys of the above example are AS41, AS21 [24]. Rare earth elements are also find a favorable option because of their solubility in Mg, which gives to another new alloying series called Mg-Al-RE [25].

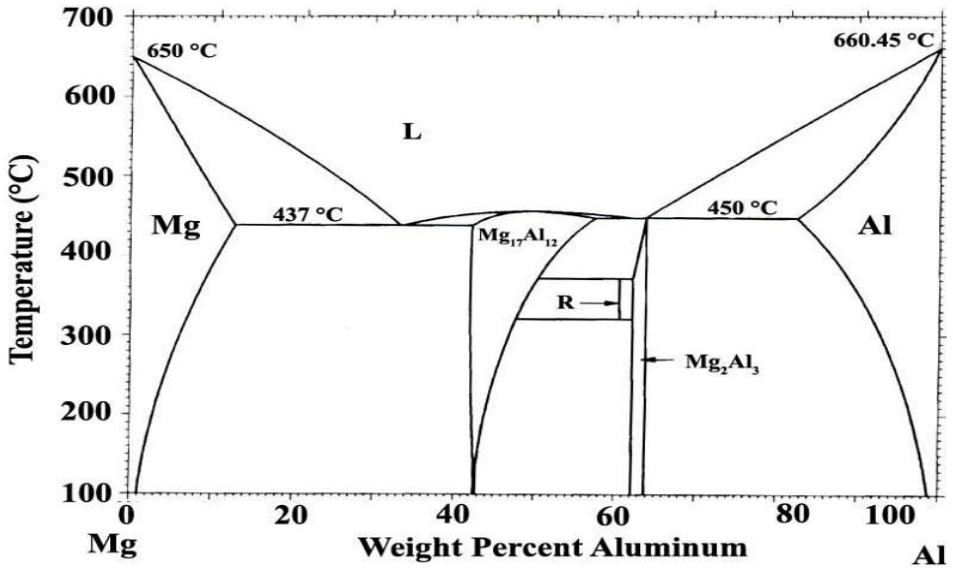

Fig 2.4 shows the phase diagram of Mg-Al system

The good example for the Mg-Al-RE is the AE42 which contains 3 wt. % of RE and 4 wt. %Al in it. AE42 is found to exhibit better creep resistance when compared to AS41 or any other Si alloying additions. [26]. But there is huge limitation in the field of rare earth alloying additions, because they are very expensive when compared to other alloying elements [24]. Researches have also analyzed the formation of the new intermetallic which is Al-RE based known as Al_4RE, and the above intermetallic is only stable until 160°C and therefore Mg-Al-RE alloying systems have been ruled out due to the above limitations and also due to temperature limitations.

So the research has been shifted towards the cheaper alloying elements, Ca is a best option because it also helps in a great extent in grain refinement [27]. It has been proved that by the addition of nearly 2.5% result in a vast increment in the creep properties of alloy in which Al is the major alloying element. But one of the major disadvantage with the use of Ca is, when it is used in excess it results in the hot cracking.

Giant automobile manufacture Volkswagen did a quality research on Ca alloying to the Mg-Al based and found out that by adding the Ca by nearly 1% to AZ81 results in superior creep properties than of the AZ81 Mg alloy. But these Mg-Al-Ca cannot be manufactured by the high pressure die casting (HPDC), because of the various problems like hot cracking, sticking to the die. However researches on the Mg-Al-Ca based has been done to control the amount of the Ca that is being added in order to obtain best suited mechanical properties [28]. From the above researches, it is observed that when the Ca content exceeds its critical of nearly 1.1% then the

alloy is subjected to cracking. Strontium is also added to the Al based Mg alloy in order to increase the creep resistance [29]. One of the examples for the Mg-Al-Sr based is AJ62 which generally contains the 6%Al and 2% Sr in it. These Sr based alloys is found to be having higher mechanical properties when compared to that of the Al base Mg binary [30]. But the draw back in this field is that the research on this Sr based Mg alloy is yet to be done in a vast extent.

2.8.2.1 Analysis of AZ91D Mg alloy

As the above mentioned AZ91D Mg alloy is the most conventional and are widely used Mg alloy in the automobile sector in room temperature applications [31]. This alloy has been finding a lot of applications because Al alloying will result in better casting capabilities and various assortment of the properties. AZ91D Mg alloy finds a variety of applications in transportation sector such as body frames, body panels, and transmission system. AZ91D is also older and a prior/chief Mg alloy ever known.

When we consider the composition in the above AZ91D Mg alloy, it comprises of 8-9% Al and 0.5-1.0 % Zn and < 0.33 % Mn. A little amount of Si and Fe can also be present. Aluminum is the prime alloying element offers good casting properties. The amount of zinc that is present will result in providing the good high temperature corrosion properties and the strengthening of the solid solution. Mn helps to nullify any effects that are present due to the iron content in it. But the above mentioned AZ91D Mg alloy has a key hindrance in creep strength at the elevated temperatures which limits its usage only to the room temperature applications [23].

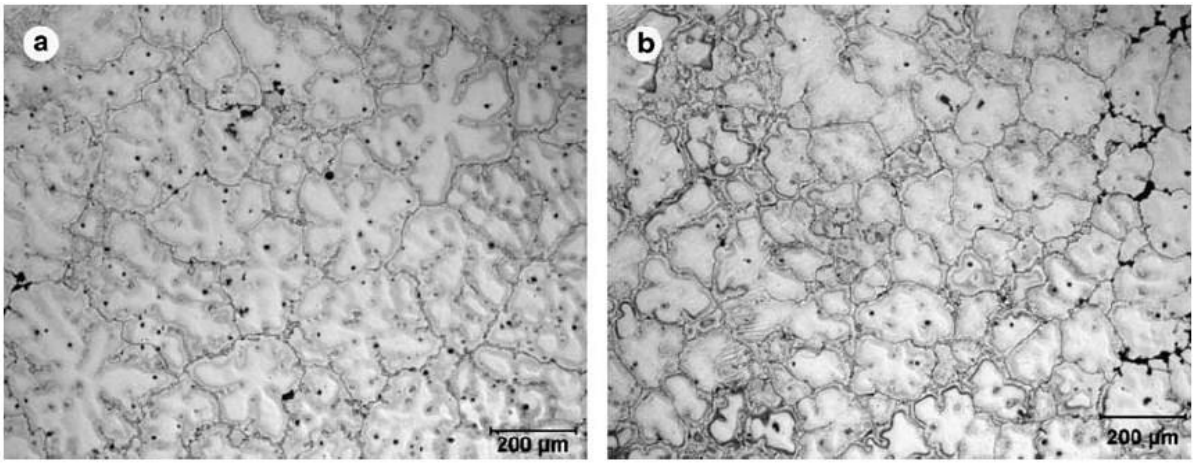

Fig. 2.5. Shows the SEM micrographs of Mg alloy with 9% Al content in it

2.8.2.2 Mg-Al-Ca based alloy system

Among all the above mentioned alloying additions, Ca has a wide scope in the research as it offers various advantageous when compared to that of the other alloying additions such as economical, high casting capability and better creep strength at the elevated temperatures. Hence the above alloy system is greatly suited for the manufacturing of the various parts in powertrain sector to increase its efficiency.Ca added Mg-Al system is used in various applications like lubricating system, body frame, cylinder covers [32]. So a vast research is going on in the Al-Ca based Mg alloy system and its deformation creep mechanisms at the superior temperatures has been observed. Various observations have stated that when the Ca is added to the Mg alloys its properties at the elevated temperatures including shows a vast improvement [33]. But later on it has been realized that if the excess amount of Ca is used which is above the critical composition of 0.45% shows the undesirable features like sticking to the die and cracking. So the applications regarding Ca based Mg alloys has been very limited due to above undesirable factors. On the recent days, researchers are focused to eradicate the undesirable features by

further more alloying the Ca based Mg alloys to improve its casting properties. [34]. Various experiments were conducted by the lou [34] and observed that by the addition of Zn which is nearly 7-8% helps to improve the casting capability of the Ca based Mg alloy with 0.5-1.5% Ca content in it. But the process by which the casting capability has been increased is yet to be known [73]. Similar observation is also been done on the AM50 Ca based Mg alloy by adding the Ca at the temperature range of 160-190°C helps to improve the casting ability. [35].

The results that are obtained previously are in completely agreement with the observations done by horie et al. [36]. A various experiments were done by powell [37] on the high Ca containing Mg alloy comprises of 5 wt. % Al. But despite of the high Ca content in the Mg alloys, he observed that there is no tearing or cracking takes place in the alloy and the creep strength at the elevated temperature has been largely increased. Powell conducted the tests on the Mg alloy comprising of 5 wt. % Al and 3 wt. % Ca which gives best suited mechanical properties at the higher temperatures. The results that are obtained by powell are also been observed by Tereda et al. [38] by conducting similar tests on the alloy with 1.8 wt. % Ca content in it. Upon the microstructural studies, it has been observed that the Ca containing Mg alloy consists of α-Mg grains which are being enclosed by the secondary/intermetallic phase. Die cast Ca based alloy provides better properties when compared to that of the permanent casting because of the variation in the grain size has been observed. It has been observed that by the Ca alloying addition the intermetallic β-$Mg_{17}Al_{12}$ phase is being diminished in the Mg alloys. But at the earlier stages of research on Mg-Al-Ca based alloys, nature and the mechanism of the formation of the intermetallic is not known completely. The above mentioned researchers such as Renaud [39] and Lou et al. [36], observed the formation of distinct and unique intermetallic known as

C36 along the grain boundaries by the various highly developed characterization (XRD and TEM) techniques. By the above techniques it has been concluded that C36 is known as (Mg, $Al)_2$ Ca. It has been observed that at as the Ca content goes on increasing, the formation of the C36 will be formed by diminishing the β phase. C36 has higher stability at the elevated temperatures and have higher melting point than that of the β phase and is effective in the pinning of the grain boundaries and simultaneously increases the creep strength of Mg alloy until 160°C [39]. Creep resistance is greatly increased with the increase in the Ca content, this is due to the fact that with increasing in Ca content, the intermetallic C36 phase has also been increased which is beneficial for creep strength at higher temperatures. Lou [36] has observed that the new intermetallic phase C36 is a die hexagonal structure and is stable at the higher temperatures than that of the β phase due to the coherency of C36 phase with α Mg grains. The increased creep resistance is due to the prevention of the grain boundary sliding by the intermetallic that encircles the grain boundaries.

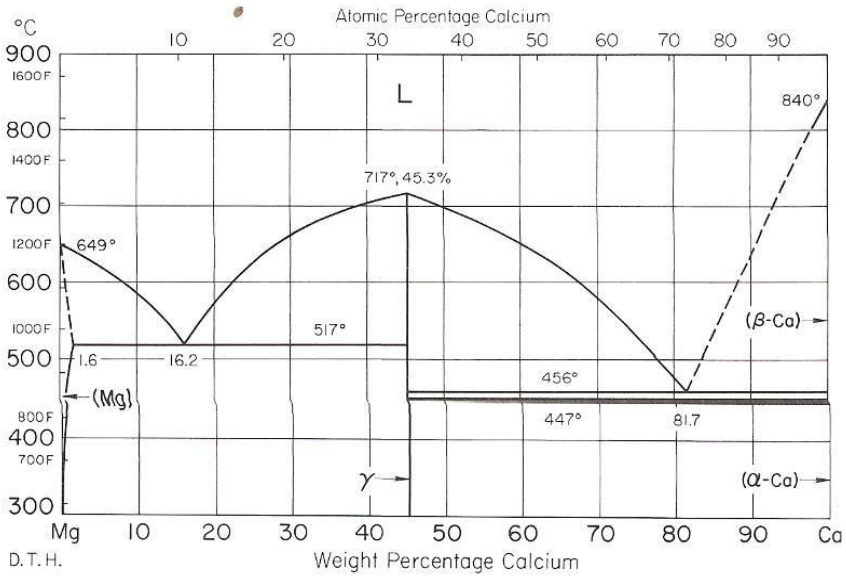

Fig. 2.6. Shows the binary phase diagram of Mg-Ca system

Recently a series of experiments were conducted by the Suzuki [40] on Mg-Al-Ca based in order to know the nature and coherency of the C36 intermetallic and its behavior in the elevated temperatures by various sophisticated techniques. He also found that the above mentioned C36 phase also exhibit di-hexagonal crystal structure and found its stoichiometric relation as $((Mg,Al)_2Ca)$ .By various creep testing observations it has been noted that the C36 phase can remain coherent until nearly 480°C. But one important observation regarding C36 is it decays to form the two similar intermetallic phases known as C15, C14 as the temperature decreases drastically below 420°C. But when the temperature and other conditions that are similar to powertrain sector is applied on Mg-Al-Ca it is observed that the transformation is taking place from C36 to C15 but it is comparatively slow. It also observed that while transforming into C15 phase, there is a possibility of spheroidal growth of intermetallic takes place at the superior temperatures and longtime of aging. Various researches also conclude that there are some particles in the intermetallic which is being reported as rich Mg regions in the Ca based Mg alloys. So by the above factors it can be observed that, by the formation of the intermetallic and diminishing of the β phase will result in better mechanical and creep properties at the superior temperatures. And these type of alloys can also be produced commercially in order extend its applications in various fields.

2.9 Creep Deformation Mechanisms

Creep is generally defined as the deformation which is of plastic in nature occurs due to the increase in the temperature which is nearly the half of the melting temperature. Creep deformation is generally occur by three unique mechanisms which occur at the grain or microstructural level. They are:

1. Dislocation creep
2. Diffusion creep
3. Grain boundary sliding (GBS)

All these unique mechanisms are in microscopic level and their occurrence is independent to each other. The deciding factors for the three mechanisms are temperature, grain size. In the grain boundary sliding, the creep occurs by sliding the grains on each other and there is a possibility in the shape of grains .

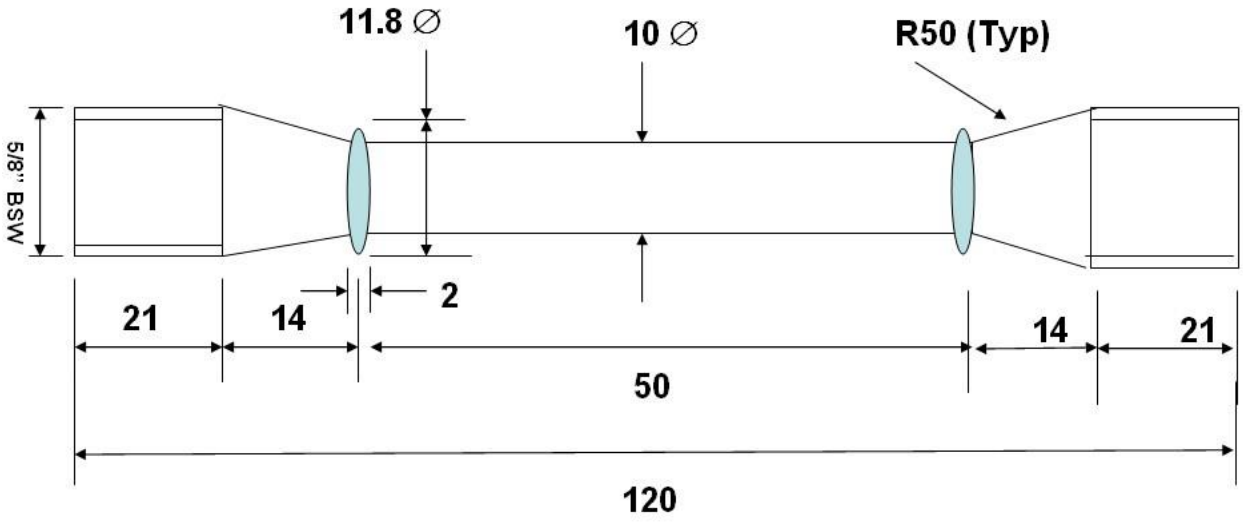

Fig. 2.7. Shows the standard creep specimen

2.9.1 Dislocation creep

In dislocation creep, the deciding factors are dislocation glide and dislocation climb. It is the plastic flow deformation which generally occurs in lattice of the grain. Here the dislocation is concentrated in lattice of the grain. The main reason for dislocation creep to takes place is the

solute atoms hinder the movement of dislocation.. The exponent of stress 'n' in the above type of solutions is around in the range of 3. These type of solid solutions are known as solutions of I class. Such kind of alloys are called class I solid solutions. The strain rate for the above dislocation creep is given by the following formula:

$$\varepsilon = AD_s\sigma^3$$

In the above equation, D_s is the coefficient of diffusion

2.9.2 Diffusional creep

Diffusion creep as the name indicates, here the deformation occurs by diffusion at the elevated temperatures. It is generally predominant in fine grain metals or alloys at the temperature range of 0.5-0.9 $T_{m.}$. Diffusion creep is generally of two types.

1. Nabarro-Herring creep
2. Coble creep.

The grain size is more controlling factor in Nabarro-Herring creep

For the Nabarro-Herring creep, the transport of matter is by lattice diffusion, while for the Coble creep, the transport of matter is by grain boundary diffusion. The Nabarro-Herring creep has less grain size dependence than Coble creep. Also, the activation energy for Nabarro-Herring creep is greater than that for Coble creep [41].

2.9.3 Grain Boundary Sliding (GBS)

It is the chief and most observed mechanism for the high temperature deformation for the most of metals and alloys. As described earlier, it is occurred by the sliding of the grains which is

responsible for the creep elongation. In this there is a possibility of the cavitation at the premature level at the most critical regions and triple points. [42]. Grain boundary sliding is more predominant in the fine grained structure, when compared to the coarse grain structure. The value of the exponent of stress 'n' should be in the range of 2-3 for the GBS to take place. GBS is a plastic flow mechanism that contains dislocation glide and dislocation climb by which the movement of dislocation take place. In GBS the energy for activation is equal to diffusion energy in grain boundary or diffusion energy in lattice. At the elevated temperature, the strain occurred by GBS can be calculated by the following :

$$\varepsilon=\varepsilon_{dc}+\varepsilon_{gb}+\varepsilon_{ipg}$$

In the above equation, ε is the total strain developed; ε_{dc} is the amount of strain contributed from dislocation creep; ε_{gb} is the creep contributed by grain boundary sliding; ε_{ipg} is the creep by inter granular process that occurs within the grains of the alloy.

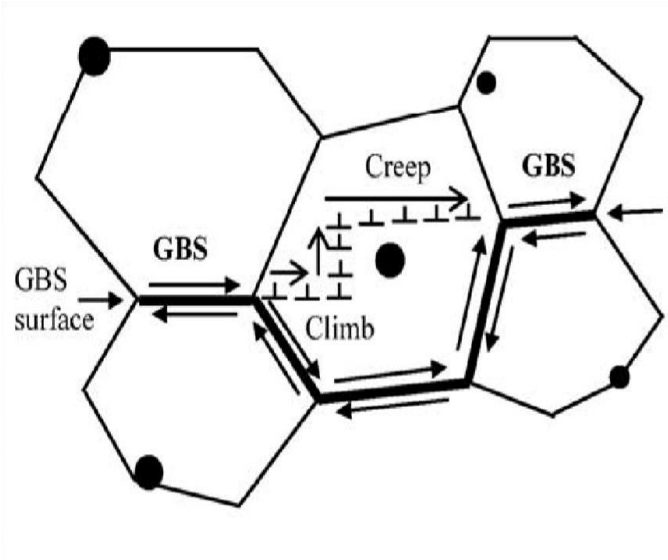

Fig. 2.8 shows the sliding of the grain boundary

2.10 Creep analysis and creep guiding mechanisms in Mg-Ca-Al based alloys

Creep deformation mechanisms is one of the significant factor that decide the creep resistance of the alloy. Hence there is a need to study the behavior of the intermetallic during the creep test in order to use for the superior temperature applications. Hence various researches has been done to study the creep behavior of Ca based Mg-Al alloy system. [43]. In order to find out the effective mechanism of creep by which the elongation happens, can be found out by using the constant 'n'. This constant 'n' is known as exponent of stress which can be derived by plotting the graph between stress and strain rates (ε) at a particular temperature. But one of the draw back with the Ca based Mg alloy systems is that the constant 'n' elaborated behavior is yet to be explored [43]. Various researches has been done to find out the value of 'n' so as to determine the crucial creep mechanism in the Ca based Mg alloys. Numerous tests has been conducted by the Tereda [38] to find out the stress component 'n' in Ca containing of nearly 1.75 wt. %, and it is found to be in the range of 9.5-10.2 at the creep testing temperature of 160 – 200 °C. He also reported that by the observation, energy required for activation (Qc) is nearly in the range of 140-150 KJ/mole. So by value of constant 'n' and the energy required for the activation, that the dislocation creep is effective driving creep mechanism in Ca containing Mg alloys [38]. It is also observed that by comparing the properties of creep before and after addition of Ca, that resistance towards creep has been increased by 2-3 times when compared to later. Other researchers like powell [36] also observed the mechanism of creep by adding trifling amounts of Sr in the Ca based Mg alloys. He observed that by calculating the constant 'n' at very different stress conditions which are in the range of 60-75 Mpa and found out the value of ''n' to be in the range of 1.6 and according to his results he obtained for the low stress values, sliding of the grain boundary is controlling mechanism in creep. But at the higher stress range which is

generally above 80 Mpa, he also observed to have similar results with value of 'n' to be in the range of 8.0-8.6 and the dislocation glide as well as dislocation climb is the predominant mechanism. As expected he also observed that new intermetallic phase in Ca based Mg-Al alloys increase the resistance towards creep. He also observed that the optimal resistance towards creep is obtained when the Sr of about 0.2 wt. % is added in it. But strontium behavior in the Ca based Mg alloy is yet to be explored further. A series of experiments were conducted by the Horie [37] on both the die and ingot cast alloys containing RE alloying element in it along with the Ca. The tests were conducted in the stress range of about 50-120 Mpa and a temperature range of 130 – 190 °C and found that die casting has superior mechanical and resistance towards creep when compared to that of ingot casting. The value 'n' that is calculated is greater in the die casting. RE alloying addition is resulted to have the grain refinement in the Mg alloy which plays crucial role in various mechanical properties at room and elevated temperatures. The creep test which is of compressive in nature, is conducted by sohn to the Mg alloy with Ca ranging from 0.3-0.8 wt. % in it. And he observed that from the results gained from creep test, that Ca doesn't have any major role in the constant 'n' which is found to be in the range of 5.5-9.4 at the temperature 150 °C. But the changes in the as cast microstructure has been observed when the Ca alloying is done in the Mg alloys. These changes are more predominant at the grain boundaries than the interiors. Various observations are done on the Mg alloys to study the strengthening of the alloys that are imparted by the precipitation when the Ca is added in it. Similar observations were done by Suzuki [44], on AXJ530 to study the precipitation effects and its factor in enhancing the resistance to creep. It has been observed that the nature and volume fraction of these precipitation also have a greater role in deformation by creep.

Chapter 3. Experimental procedure

Table 1 depicts the chemical compositions of the aforementioned Magnesium (Mg) alloys which are formulated by inductively coupled plasma optical emission spectrometry. The cast dimensions after the material is through the Cold chamber high pressure die casting machine are 19mmX179mm in cylindrical form. On further machining the rods by spark erosion technique, the creep specimens with the dimensions 6mmX19mm are obtained. The creep tests are performed in compression with a lever arm (ratio 10:1), 'ATS' creep set-up (Model 2230), at a constant stress (70 MPa), at different temperatures for about 50 hrs. The test temperature is maintained at precisely 2°C during the creep test. The microstructures of the HPDC Mg alloys are examined using a field emission scanning electron microscope (FESEM) (Model: FEI Sirion XL30) equipped with an energy dispersive X-ray spectroscopy (EDS) analysis. The samples for the test are prepared by standard techniques of metallography. A solution of 100 ml ethanol, 10 ml acetic acid, 6 ml picric acid and 20 ml of distilled water is used for etching

Element (wt. %)	Alloy		
	AZ91D	MRI153M	MRI230D
Al	9.02	7.95	6.45
Ca	-	0.98	2.25
Zn	0.84	<0.01	<0.01
Mn	0.23	0.20	0.27
Sr	-	0.27	0.25
Sn	-	<0.01	0.84
Mg	Balance	Balance	Balance

Chapter 4. Results and Discussion

Fig. 4.1 represents the XRD patterns obtained from all the alloys employed in the present investigation. It is obvious that peak corresponding to α-Mg is present in all the alloys. In addition, the AZ91D alloy contains peak corresponding to $Mg_{17}Al_{12}$ (also known as β phase) phase, MRI153M alloy contains $Mg_{17}Al_{12}$ and C36 ($(Mg, Al)_2Ca$) phases and MRI230D alloy contains C36 ($(Mg, Al)_2Ca$) phase. The $Mg_{17}Al_{12}$ phase is generally present in Mg-Al alloy and it get suppressed with increasing content of Ca. Therefore, $Mg_{17}Al_{12}$ phase was fully absent in MRI230D alloy having 2 wt.% Ca although it is present slightly in MRI153M alloy having 1 wt.% Ca.

4.1. As cast microstructure

Fig. 4.2 displays the FESEM micrograph of the HPDC AZ91D alloy. From the micrograph, we can observe that the intermetallic $Mg_{17}Al_{12}$ having melting point of 437°C is formed along the grain boundaries. This intermetallic is generally found in the Mg-Al based alloy. Along with the intermetallic phases which is of light contrast, there are some Al-Mn rich regions also observed in the figure. EDS analysis were also conducted on the AZ91 Mg alloy near the grain boundaries and the intermetallic regions. The results obtained from these regions (displayed in Fig. 4.3) were found to consist of 57.6 at. % Mg, 40.2 at. % Al and 2.1 at. % Ca which is $Mg_{17}Al_{12}$ (β phase). From the figure 4.2 we can understand the various networks of β phase and Al-Mn rich regions.

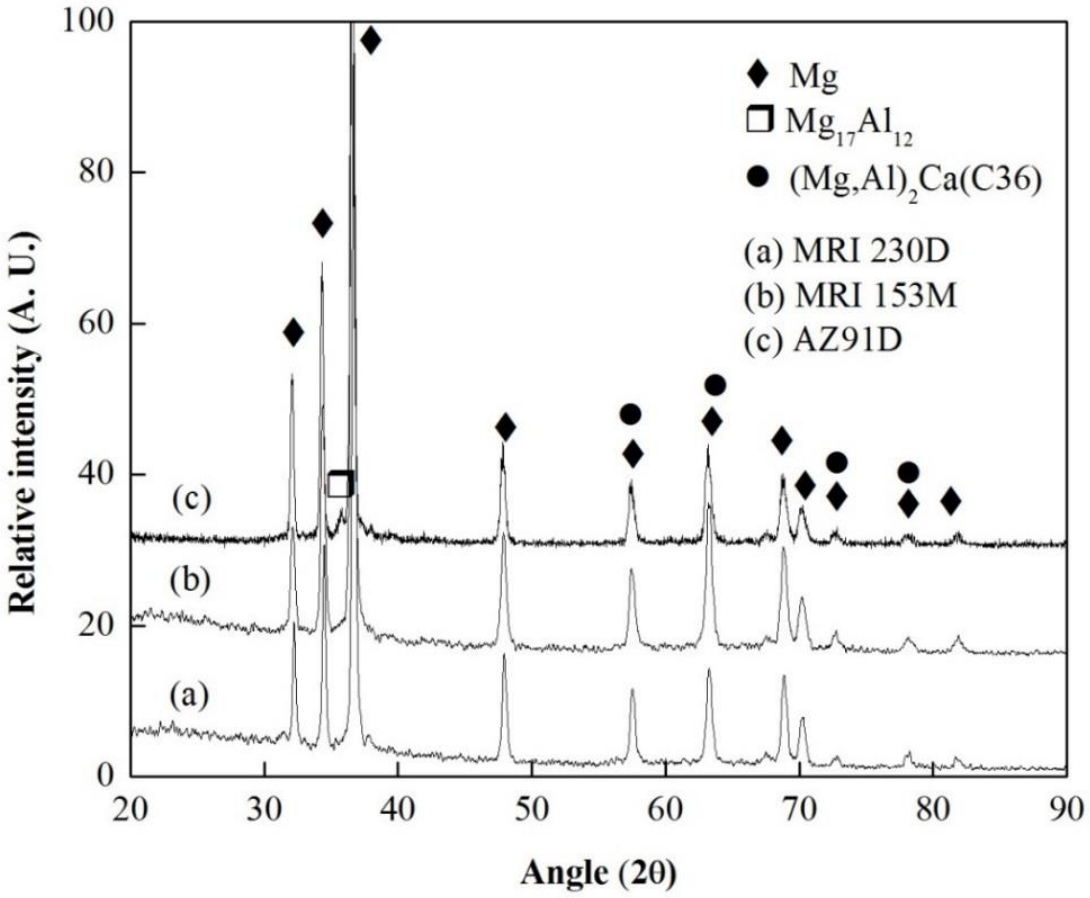

Fig. 4.1 XRD pattern for AZ91D, MRI153M MRI230D

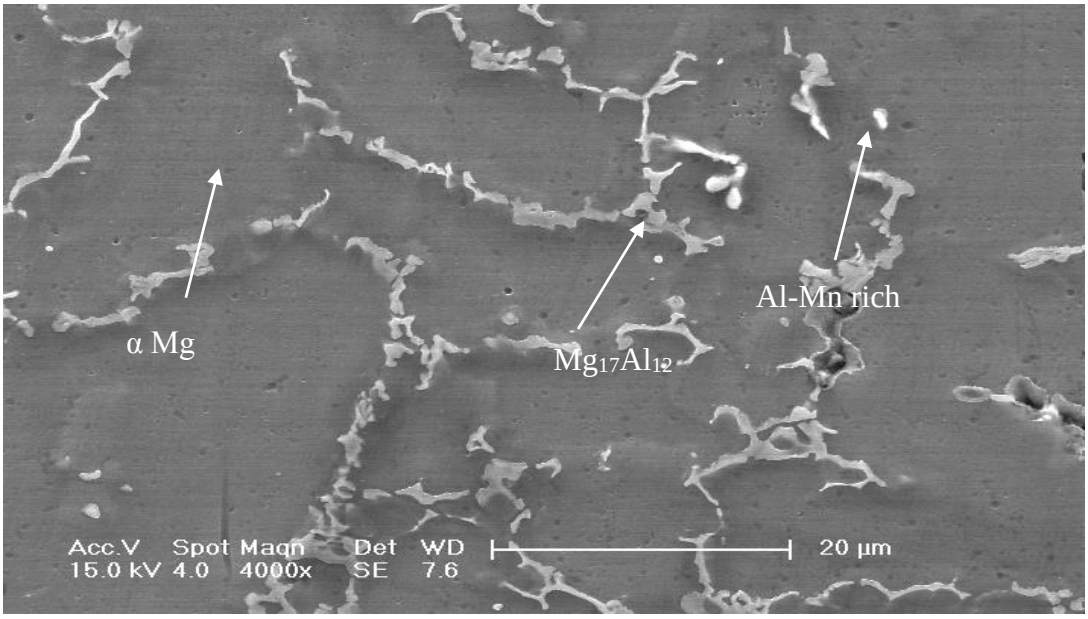

Fig. 4.2 shows SEM micrograph of AZ91D Mg alloy

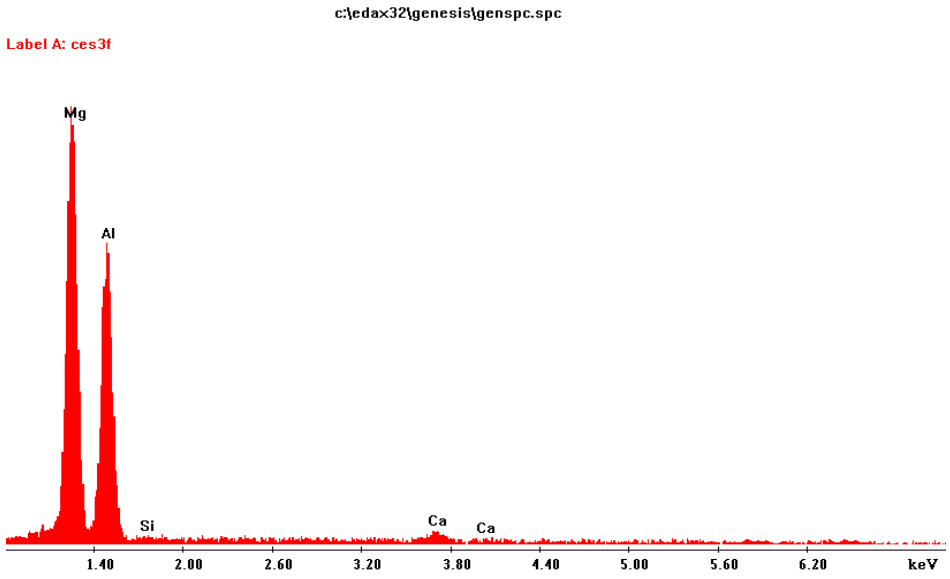

Fig. 4.3 shows EDS analysis of β phase of AZ91D Mg alloy

Ni et al. [45] conducted various SEM analysis and observed the similar results of having an Mg-Al based intermetallic network along the grain boundaries along with Al-Mn high concentrated regions in AZ91D Mg alloy. He also stated that the intermetallic present along the grain boundaries are of lamellar in nature. Dorothea et al. [46] and Yu et al. [47] too observed the $Mg_{17}Al_{12}$ intermetallic in the AZ91D alloy. Srinivasan et al. [48] also figured from various SEM micrographs that AZ91 intermetallic consists of the amalgam of two phases (α+β) precipitates with EDS observation of 67.93 at. % Mg, 28.13 at.% Al. Amira et al. [49] figured that some Al8Mn5 particles are observed which is of Al-Mn rich along with intermetallic $Mg_{17}Al_{12}$ and α Mg grains.

Fig. 4.4 displays the scanning electron micrograph of the HPDC MRI153M alloy. Unlike the AZ91D some unique and distinct features are observed in the MRI15M Mg alloy. MRI153M Mg alloy consists of the two phases encircling the α-Mg grains. With the increase in the Ca content in the MRI153M Mg alloy suppresses the formation of the $Mg_{17}Al_{12}$ phase and gives rise to formation of the new phase ($(Mg, Al)_2Ca$) C36 phase. It can be observed from the SEM Micrograph that these two phases have two different contrasts. The volume fraction of the $Mg_{17}Al_{12}$ phase is larger in the AZ91D Mg alloy when compared to that of the MRI153M Mg alloy. In the MRI153M Mg alloy, the ($(Mg, Al)_2Ca$) phase is found to be larger volume fraction when compared to that of the $Mg_{17}Al_{12}$ phase. The ($(Mg, Al)_2Ca$) phase is found to have lamellar type and bright contrast whereas the $Mg_{17}Al_{12}$ phase is found to be having the dull contrast. The C36 is found to be having the double hexagonal crystal structure having the increase in the lattice parameters with the increase in temperature. Terbush et al. [50] also observed the similar microstructure in the alloy MRI153M. Dorothea et al. [46] observed from his various alloying methods that as the alloying of the Ca increases in the Mg alloy, the $Mg_{17}Al_{12}$ phase is gradually

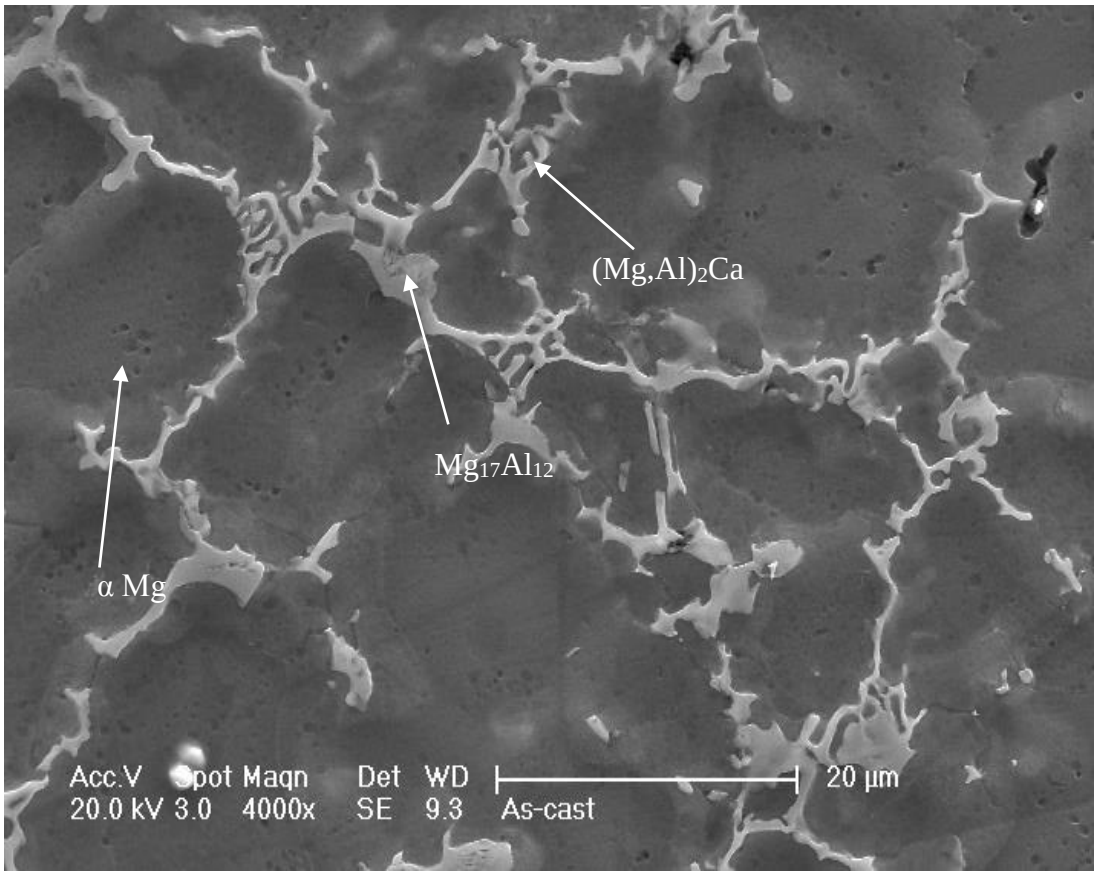

Fig. 4.4 shows SEM micrograph of MRI153M Mg alloy

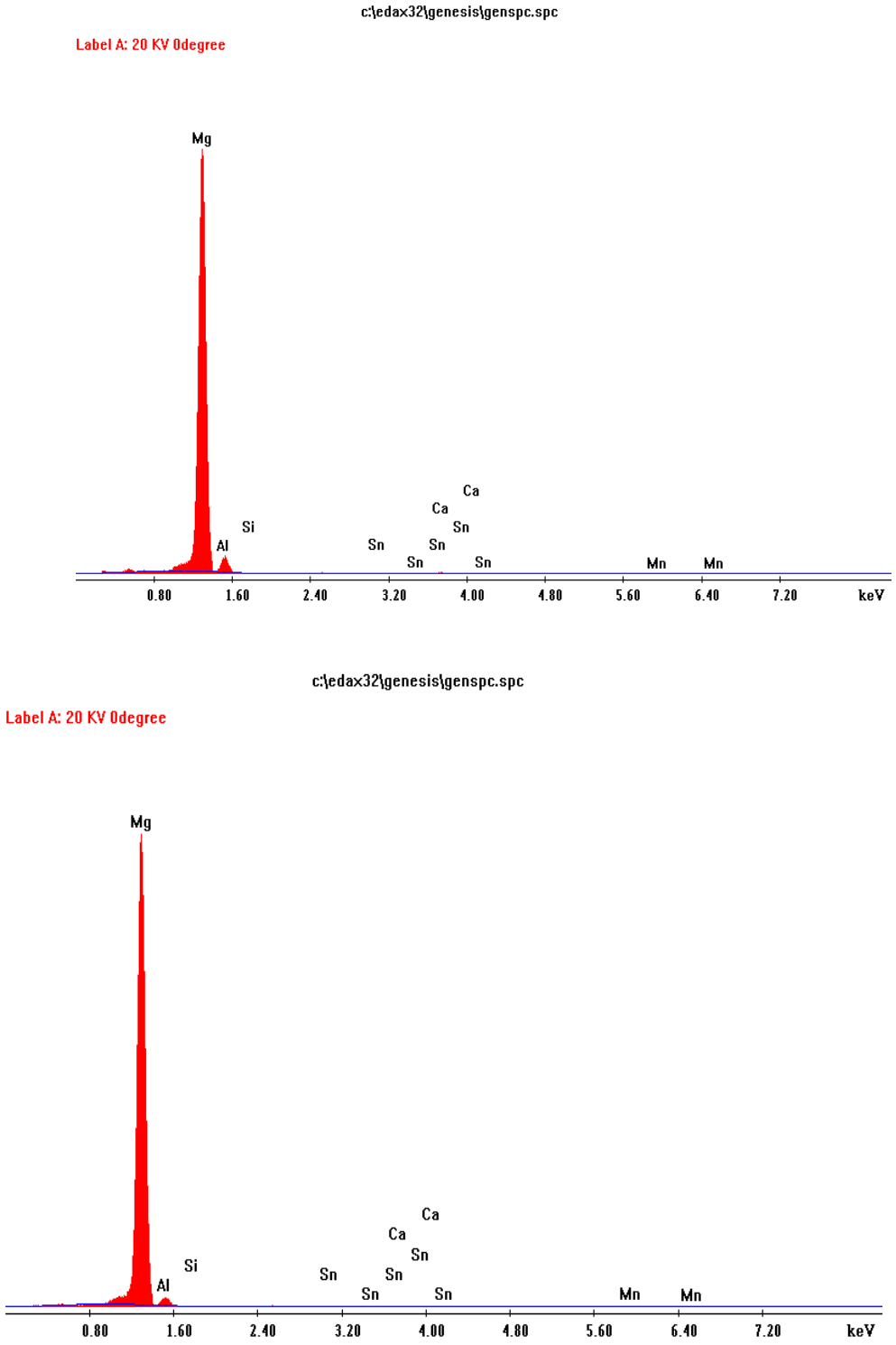

Fig. 4.5 shows EDS anlysis of MRI153M Mg alloy (a) grain interior (b) near inter lamellar region

diminishes with the formation of new intermetallic phase. Zhu et al. [49] and Amira et al. [51] also figured from SEM micrographs of MRI153M that there is an amalgam of two phases present in the MRI153M which is a mixture of $Mg_{17}Al_{12}$ phase and C36 phase. EDS analysis from the grain interior displays the results 97.2 at. % Mg, 2.6 at. % Al which is displayed in the Fig. 4.5(a) are corresponding to α-Mg. Similar EDS analysis were carried out on the MRI15M Mg alloys on the various inter lamellar regions displays the readings as 96.8 at. % Mg, 3.1 at. % Al. as shown in Fig. 4.5(b) and confirms α-Mg phase. Sato et al. [53] also did EDS analysis on the AZ91D Mg alloy on the Mn rich regions which gives a composition of 0.25 wt.% Mn, i.e., 57.0 at.% Al, 35.1 at.% Mn and 7.8 at.% Mg and matches with that of the present alloy.

Fig. 4.6 displays the FESEM micrograph of HPDC MRI230D alloy. Due to the presence of high Ca content, the β phase is completely suppressed in the MRI230D Mg alloy. Hence the intermetallic that encircles the α-Mg grains is the high melting point C36 phase (which is shown in Fig 4.6). Along with the C36 phase that is present, some Sn rich regions are also observed. The C36 phase is found to have lamellar structure. The β phase is completely absent in the MRI230D Mg alloy and the presence of the high melting point C36 phase generally results in the effective pinning of the dislocations. This results in better resistance towards creep in MRI230D alloy at the elevated temperatures. EDS is carried out on the intermetallic phase present along the grain boundaries of MRI230D Mg alloy shows 39.8 at. % Mg, 37.2 at. % Al and 18.1 at. % Ca and confirms C36 phase. Yang et al. [54] too figured out the presence of new intermetallic in Mg-Al-Ca based alloy with the increase in Ca content in the Mg-Al alloys by diminishing β phase.

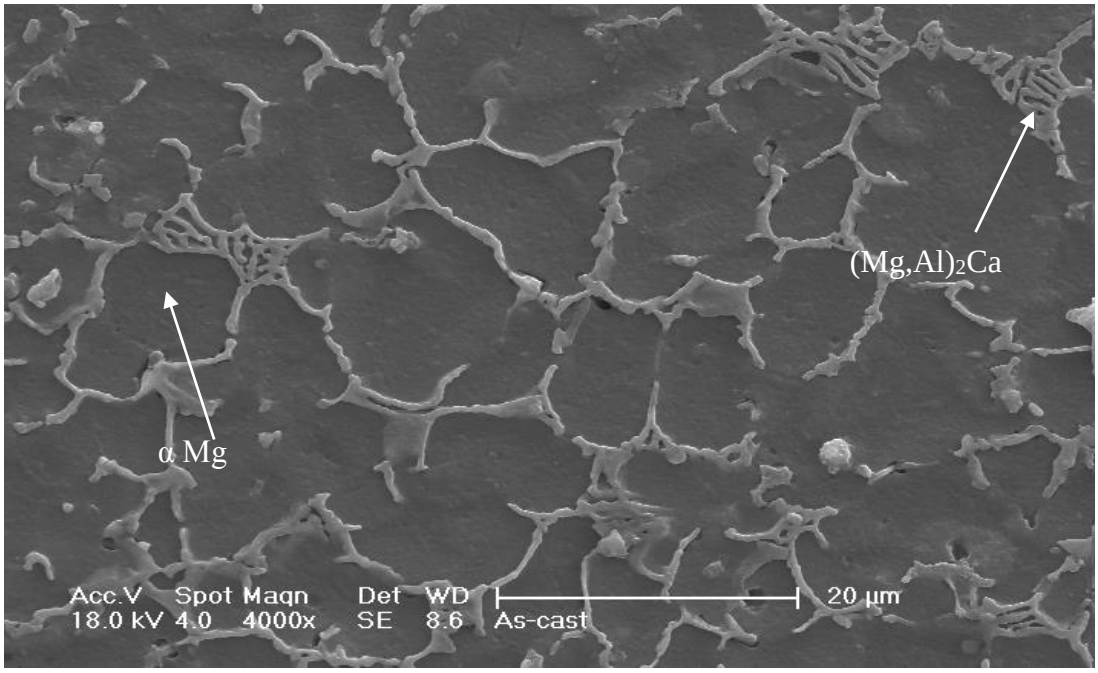

Fig. 4.6 shows SEM micrograph of MRI230D Mg alloy

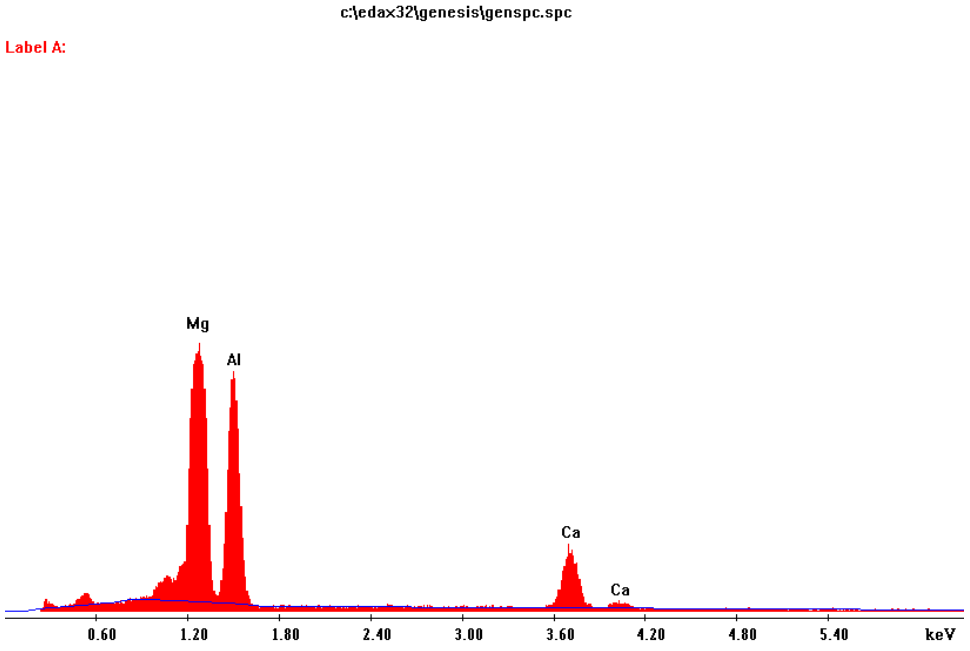

Fig. 4.7 shows EDS analysis of MRI230D Mg alloy at C36 phase

4.2 Creep behaviour

Fig. 4.8 displays the creep curves obtained from the creep tests on the AZ91D alloy conducted at 70 Mpa stress and at the test temperature of 100^0C and 150^0C continuous for 50h. From the figure it can be seen that all the creep curves have distinct primary stage followed by secondary stage. The primary stages are nearly in the range of 10-15% of the total creep test duration. The creep rates of the AZ91D alloy calculated corresponding to Fig. 4.8 is shown in the Fig. 4.9. The strain rates of the AZ91D alloy is calculated using straight line fit at different temperatures. The creep rate obtained from AZ91D at 100^0C i.e., 1.11×10^{-7} sec^{-1} is comparatively low when we compare the same creep rate at 150^0C i.e., 3.89×10^{-7} s^{-1}. There is an increase in the creep rate by a factor 3.50 when the temperature is increased by 50^0C. Hence, AZ91D alloy is only suitable up to 100^0C. As the temperature increases above it, significant elongation in creep has been observed. Srinivasan et al. [48] after conducting various creep tests, observed that the creep rate for the 0.5 wt. % Sb added AZ91D alloy was in the range of 0.671×10^{-7} s^{-1} - 0.748×10^{-7} s^{-1}. In the AZ91D alloys, the intermetallic that encircles the grain boundaries is β phase which is having low melting point. Hence, as the temperature increases. The β phase softens rapidly across grain boundaries and promotes the grain boundary sliding, which increases creep elongation very rapidly.

Fig. 4.10 displays the creep curves for the Ca containing MRI153M and MRI230D alloys tested at a stress level of 70 MPa and at the temperatures of 150^0C and 200^0C for the time duration of 50h. Fig. 4.11 shows the respective creep rates of the alloys calculated from straight line fitting procedure. From Fig 4.11 it can be seen that the MRI230D is showing the higher resistance towards

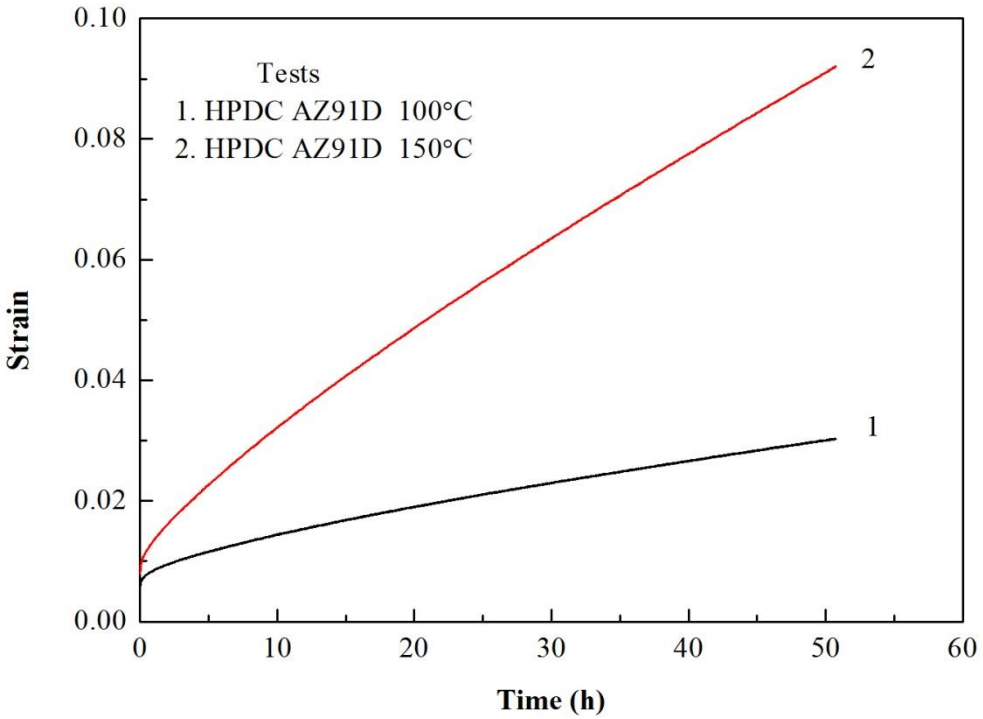

Fig. 4.8: Strain vs. time plot for AZ91

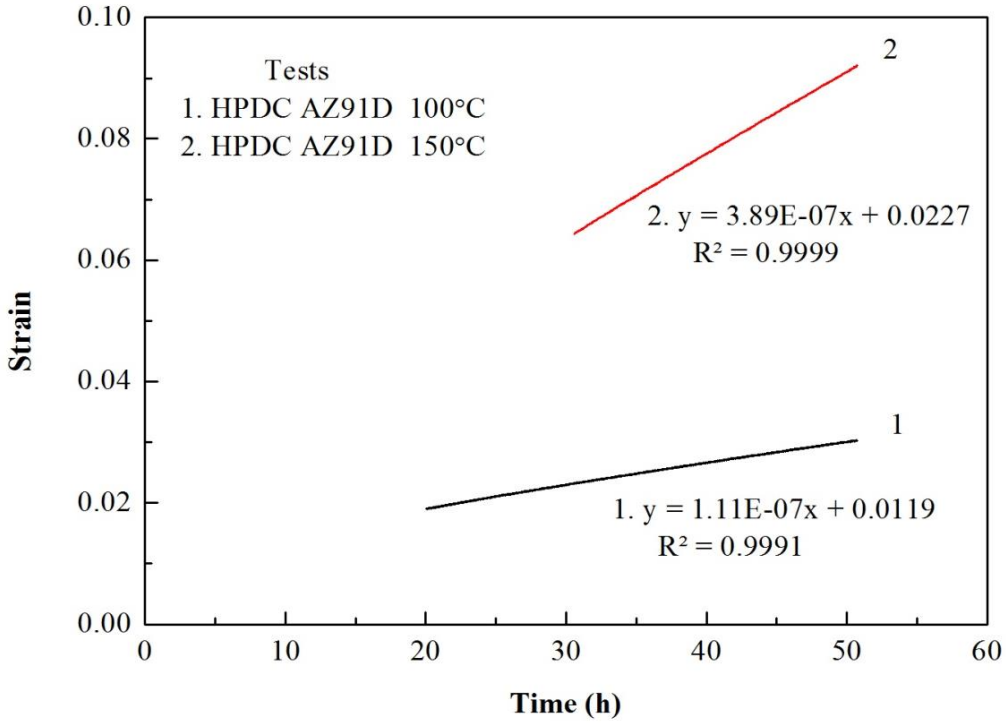

Fig. 4.9: Calculation of strain rate from strain vs. time plot for AZ91

creep when compared to that of the MRI153M. The creep rate for the MRI153M alloy is found to be $1.67\times10^{-8}\ s^{-1}$ at temperature of 150^0C. However, as the creep temperature is increased to 200^0C a drastic changes in microstructural happens, and the creep rate is found to be $3.89\times10^{-7}\ s^{-1}$ at 200^0C. The creep rate was increased by a factor of nearly 23.2. It is also observed that the creep rate of AZ91D alloy at the temperature of 150^0C is found to be nearly equal to the creep rate of MRI153M Mg alloy at 200^0C (i.e. $3.89\times10^{-7}\ s^{-1}$). Similarly, Fig. 4.11 shows the creep rate of MRI230D alloy tested at the temperature of 200^0C for 50h at a stress level of 70 MPa. From Fig. 4.11 by straight line fit, the creep rate of MRI230D Mg alloy is found to be $5.55\times10^{-8}\ s^{-1}$ at 200^0C which is lower than that of the MRI153M at the same temperature by the factor of 7.0. From the statements, we can conclude that MRI230D alloy is more resistance towards creep when compared to AZ91D and MRI153M under similar set of conditions. From the creep rate curves, we also can conclude that, the rate of creep observed in MRI230D at the temperature of 200^0C (i.e. $5.55\times10^{-8}\ s^{-1}$) is nearly half when compared to the rate of creep in AZ91D (i.e. $1.11\times10^{-7}\ s^{-1}$) under similar set of conditions at 100^0C. This can be properly explained by the precipitation and coarsening of the β phase in AZ91D and MRI153M alloys as the temperature increases. Mondal et al. [55] conducted a series of creep tests and obtained similar range of creep strain rates for the both MRI153M and MRI230D alloys. Terbush et al. [50] too reported creep rates of same order ($2.73\times10^{-8}\ s^{-1}$) for the MRI230D alloy at temperature of 180^0C. The C36 phase present in the MRI230D alloy do not soften at high temperature and resists dislocation movement during creep deformation. Therefore, it can be stated that the MRI230D Mg alloy can be used for superior temperature applications when compared to the AZ91D and MRI153M Mg alloys.

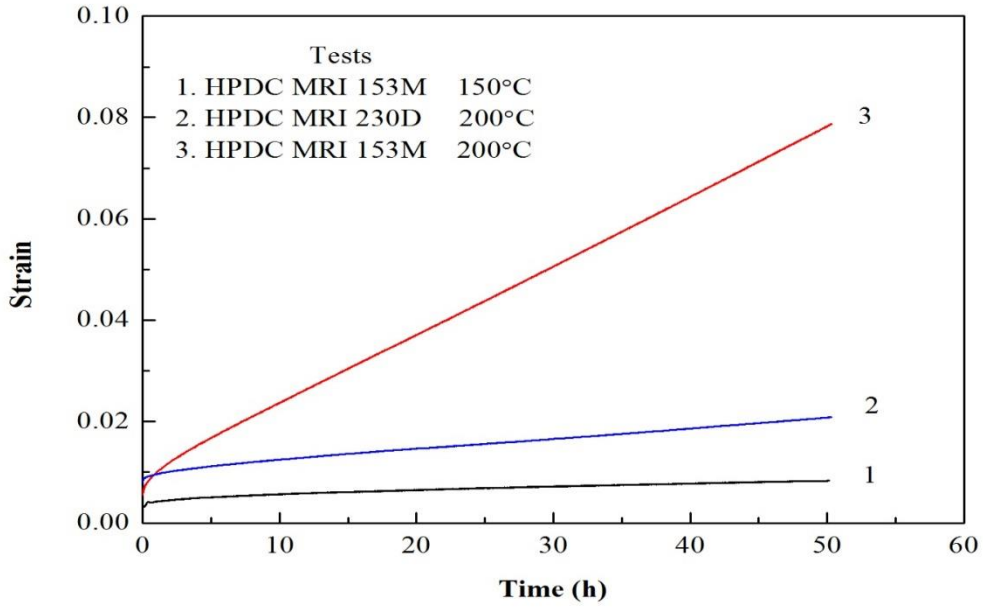

Fig. 4.10: Strain vs. time plot for MRI230D alloy

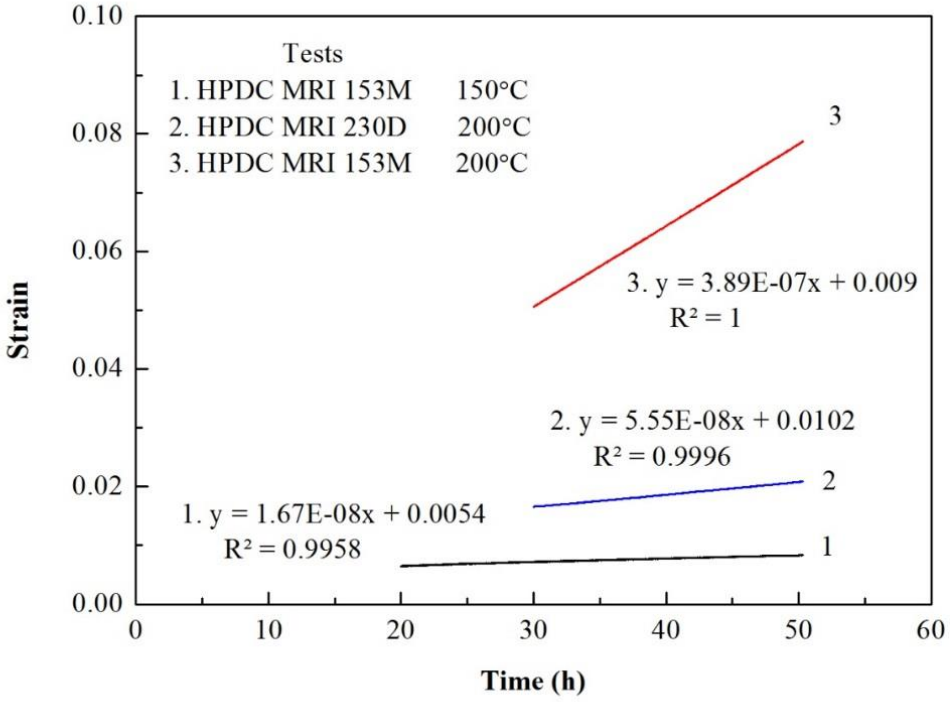

Fig. 4.11: Calculation of strain rate from strain vs. time plot for MRI230D alloy

4.3 Microstructural changes following creep tests

Fig. (4.12-4.14) below displays the various Scanning electron micrographs of the AZ91D,MRI153M, MRI230D Mg alloys after the creep testing at different temperatures. Fig. 12(a-b) displays Scanning electron micrographs of the AZ91D sample after creep testing at the temperatures of 100^0C and 150^0C for the time duration of 50h. Major difference that is observed is the volume fraction of the intermetallic phases that encircles along the α-Mg grains. The volume fraction of the intermetallic β phase is higher in specimen tested at 150^0C when compared to that of the specimen tested at 100^0C. This can be explained by the precipitation of β phase along the grain boundary regions with increase in temperature. JI et al. [56] too observed the same results when creep tested on the rheo die cast of the AZ91D Mg alloy. They observed that precipitation initiates in the regions near the grain boundaries. The amount of precipitation increases when the duration of the creep testing increases or when the alloy is being subjected to the superior temperature. As the creep testing progress the eutectic $Mg_{17}Al_{12}$ phase gradually divorce and resulting into discontinuous precipitates in the critical regions and along the grain boundaries. Dorothea et al. [46] also observed that the precipitation generally initiates in the regions where Al saturation is more predominant, which is generally along the grain boundaries. It is observed from Fig. 12(b) that the amount of β-phase at the grain boundaries has increased in the AZ91D alloy after creep test. It is also observed that after creep testing, it is only the β-phase at the grain boundaries that has increased, as shown in Fig. 12(a–b). It is evident that apart from the increment in the intermetallic there is no formation of any new phases. Kubasek et al. [57] also stated that during creep testing of AZ91D alloy the non-coherent β-phase precipitates from the Al supersaturated regions. Due to thE precipitation of β-$Mg_{17}Al_{12}$ phase in AZ91D, there is a slight increase, in the hardness of the alloy, which is good for creep resistance.

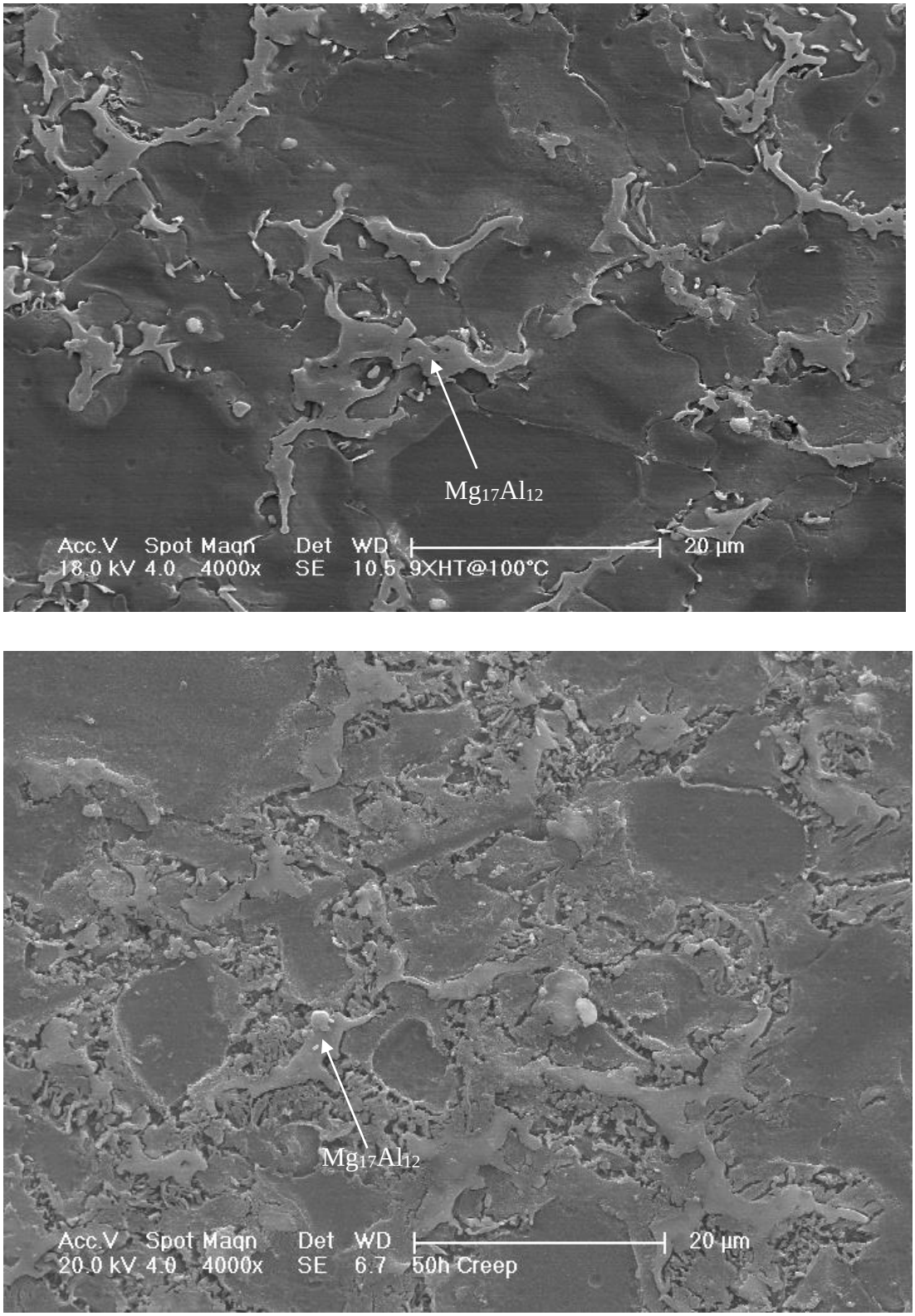

Fig. 4.12 shows SEM micrographs of AZ91D alloy creep tested at (a) 100^0C (b) 150^0C

Fig. 4.13(a-b) shows the Scanning electron micrographs of the MRI153M Mg alloy creep tested at the temperatures of 150^0C and 200^0C at a stress level of 70 MPa for 50h duration. As in the case of AZ91D, MRI153M also has a prominent change in the volume fraction of the intermetallic encircling the α-Mg grains. From the figures shown in 4.13(a) and 4.13(b) it is observed that only the volume fraction of the β phase increases considerably, whereas the volume fraction of the C36 phase remains unaffected. As mentioned earlier, that the β phase softens and coarsens as the creep testing progresses and is the major cause for lowering of creep resistance of the MRI153M alloy.

Fig. 4.14 shows the Scanning electron micrograph of the HPDC MRI 230D alloy after Creep testing at 200^0C and 70MPa for 50h. It is been observed that the volume fraction of the intermetallic phase C36 after creep testing, increases as compared to the as cast MRI230D Mg alloy. The amount of the C36 phase depends mainly on the duration of the creep testing and temperature. Terbush et. Al. [50] too stated that the creep resistance in the MRI230D is higher when compared to that of the MRI153M alloy. The creep behaviour of as-cast MRI230D alloy strongly depends on the network of its eutectic phase solidifying in the inter-dendritic channels. When this is highly interconnected a significantly higher creep strength results. However, the temperature and time involved in the present investigation are lower and no change in the nature of C36 phase is observed after heating or the creep tests

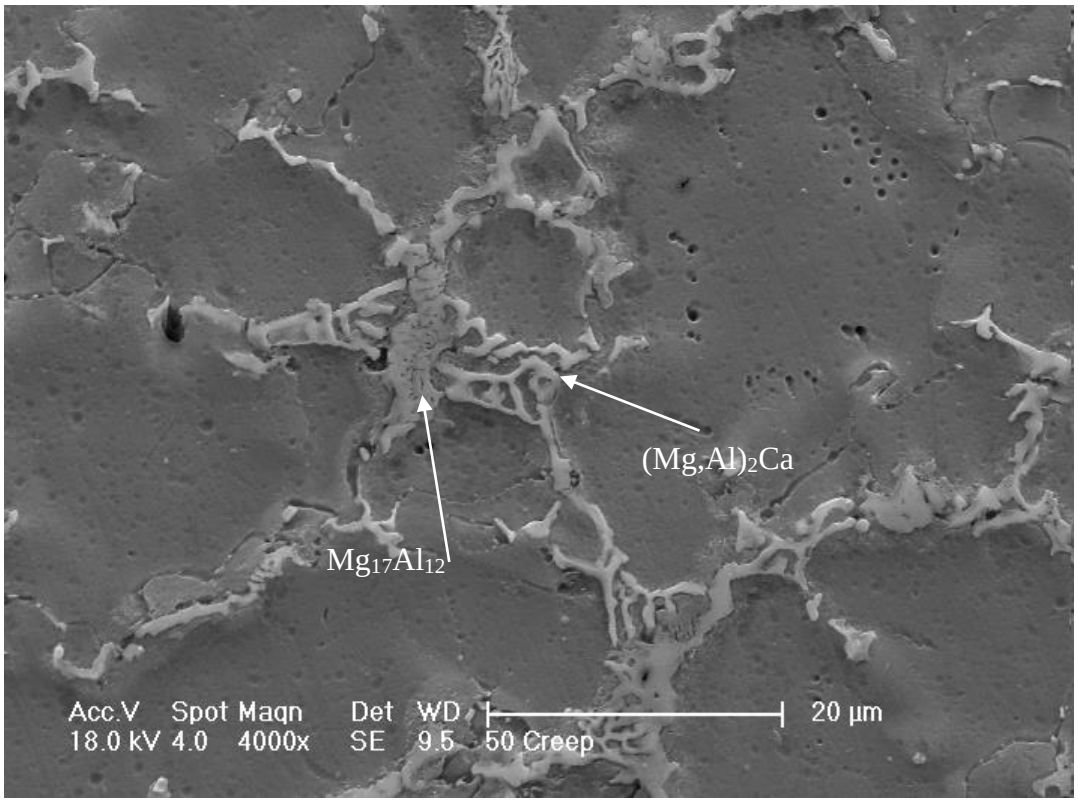

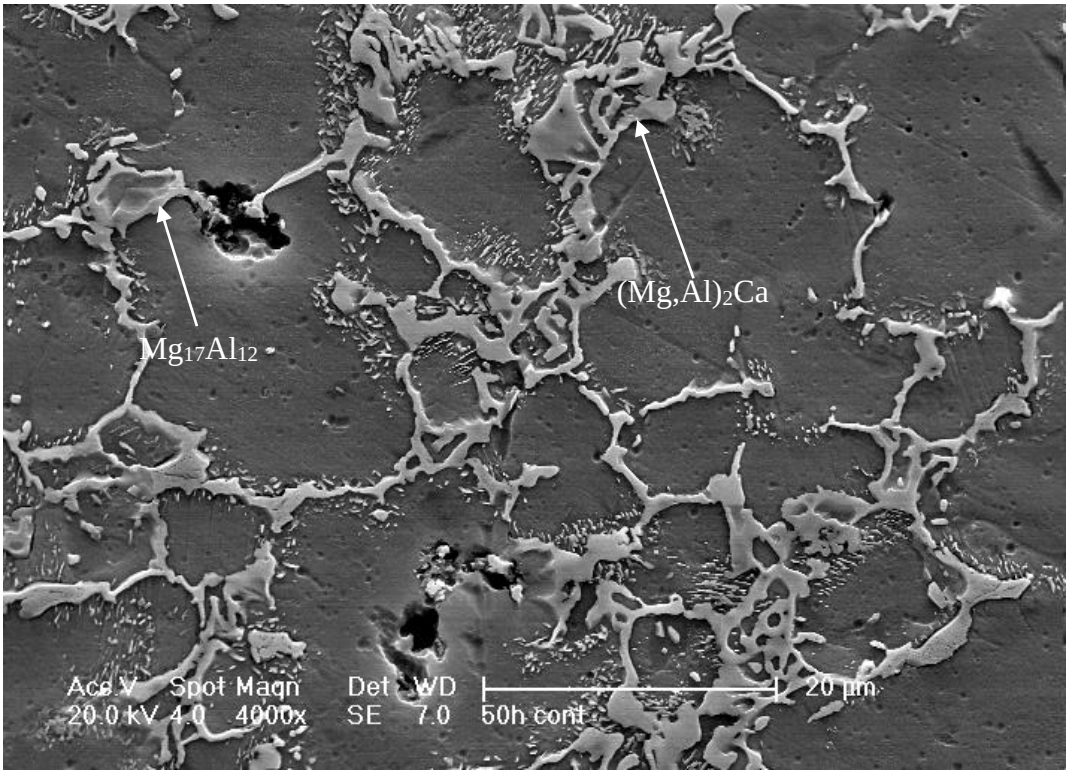

Fig. 4.13 shows SEM micrographs of Creep tested MRI153M alloy (a) 150^0C (b) 200^0C

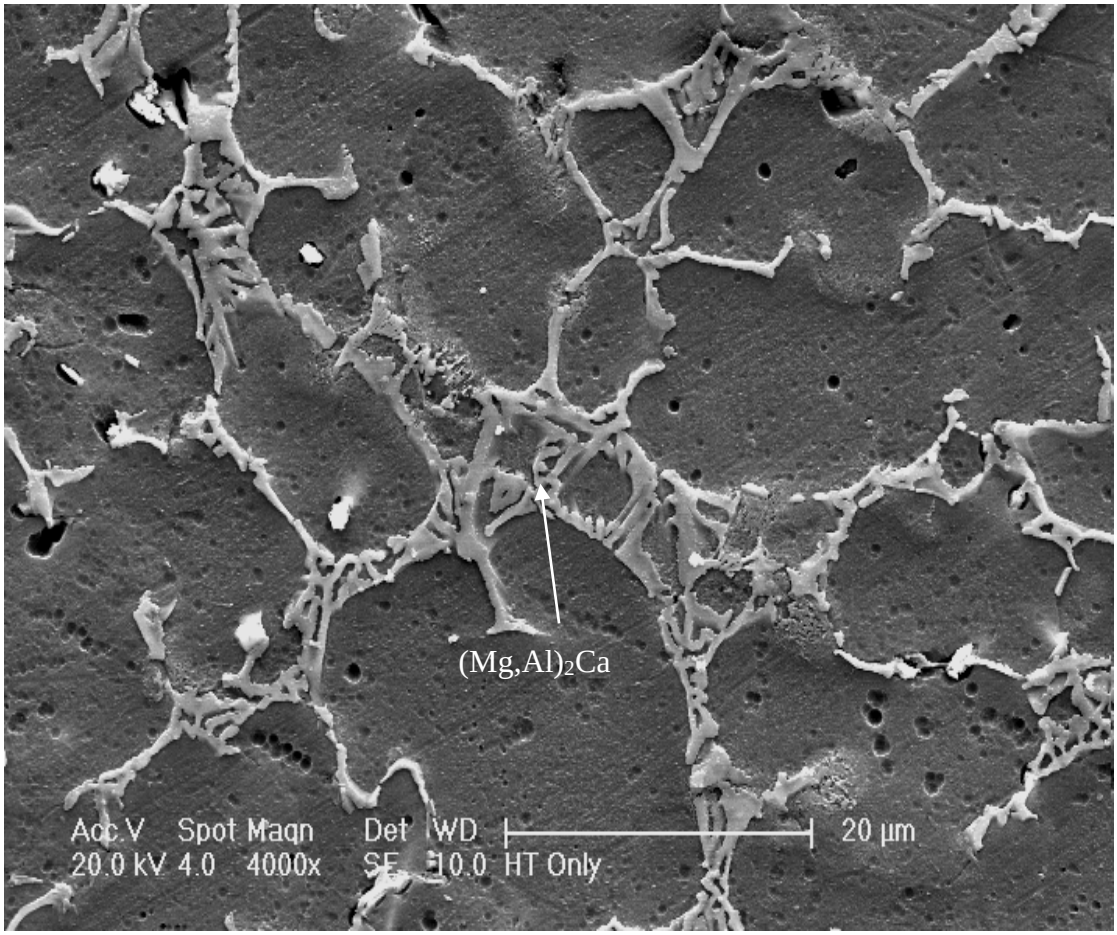

Fig. 4.14 shows SEM micrographs of Creep tested MRI230D alloy at 200^0C

.

Thus, from the above statements, we conclude that during the creep testing of the three Mg alloys at different temperatures doesn't result in the formation of any new phases along the grain boundaries. It only result in the precipitation of the existing intermetallic phases. In case of AZ91D and MRI153M the precipitation of β-$Mg_{17}Al_{12}$ result in the decrease of the creep resistance of the alloy due to its low melting point whereas in the case of MRI230D, the precipitation of C36 phase results in the increase of creep resistance of the Mg alloy.

5. Conclusions

The role of the intermetallic on the creep behavior of the Mg-Al-Ca based alloys was investigated. A detailed microstructural characterization is done on the AZ91D, MRI153M and MRI230D alloys at the as cast stage and at the creep tested stage. Creep tests were done on all the three alloys at different temperatures at 70MPa stress and 50h duration. Microstructural changes followed by creep test is analyzed in all the three alloys. The following conclusions are arising out of the present investigation

- As cast microstructure of AZ91D alloy consists of α-Mg, $Mg_{17}Al_{12}$ phase along the grain boundaries whereas MRI153M alloy consists of α-Mg, $Mg_{17}Al_{12}$ and $((Mg,Al)_2Ca$. As cast MRI230D alloy consists of α-Mg and $((Mg,Al)_2Ca$.
- MRI230D alloy exhibits highest creep rate and AZ91D exhibits lowest creep rate with MRI153M alloy exhibiting medium creep rate.
- In the AZ91D alloy, $Mg_{17}Al_{12}$ phase increases after creep test and in MRI153M alloy there is an increase in $Mg_{17}Al_{12}$ phase and C36 phase remains unaffected. In the MRI230D alloy there is an increase in the C36 phase after creep test.
- The increase in the volume of $Mg_{17}Al_{12}$ phase in both AZ91DDD and MRI153M alloys decreases the creep resistance at the elevated temperatures whereas in the MRI230D alloy, increase in the volume of C36 phase after creep test improves the creep resistance

References

[1] H.E. Friedrich, B.L. Mordike, 52 (2006) 665.

[2] G.V. Raynor, (1959) 531.

[3] R.S. Busk, 188 (1950) 1460-1464.

[4] J. Sarennah, P. Longworth, (2001).

[5] http://www.vda.de/en/arbeitsgebiete/leichtbau/index.html (last accessed on Feb 2nd 2009)

[6] http://www.americanchemistry.com/s_plastics/hands_on_plastics/intro_to_plastics/students.html#history. (last accessed on Dec 14th 2012)

[7] http://www.thenewsteel.com. (last accessed on July 22nd 2010)

[8] Wilson, K. Clause, M. Earlam, J. Hillis, (1995) l.

[9] M. Henstock, (1966) 213.

[10] T.G. Nieh, J. Wadsworth, O.D. Sherby, (1997).

[11] Magnesium Electron Limited, Magnesium alloy database, MATUS Databases, Engineering Information Co. Ltd, (1992).

[12] D. Eliezer, E. Aghion, F.H. Froes, 5 (1998) 201

[13] A.K. Dahle, D.H. St John, G.L. Dunlop, 24 (2000) 167.

[14] E.F. Em1ey, (1966) 925

[15] M.O. Pekguleryuz, M.M. Avedesiaan, Sainte-Foy, B.L. Mordike, F. Hehmann, (1992) 213

[16] P.L. Schaffer, Y.C. Lee, A.K. Dahle, (2001) 8l.

[17] A.K. Dahle, Y.C. Lee, D. Nave, P.L. Schaffer, H. David, 1 (2001) 61.

[18] O. Lunder, T.Kr. Aune, K. Nisanciogluz, 43 (1987) 29

[19] B.L. Mordike, F. Hehmann, (1992) 201

[20] Z.P. Luo, D.Y. Song, S.Q. Zhang, 230 (1995) 109

[21] M. Suzuki, H. Sato, K. Maruyama, H. Oikawa 252 (I998) 248

[22] P. Abachi, A. Masoudi, K. Purazrang, 435-439 (2006) 653.

[23] P. Bakke, H. Westengen, 5 (2003) 879.

[24] M.O. Pekguleyuz, 350-351 (2000) 131.

[25] G. Foersterz, 7th International Die casting Congress, (1972)

[26] B.R. Powell, V. Rezhets, M. Balogh, R. Waldo, (2001) 175.

[27] H.J. Fuchs, UK Patent, 847 (1960).

[28] M.O. Pekguleryuz, A. Luo, (1996).

[29] M.O. Pekguleryuz, E. Baril, (2001) l 19.

[30] P. Labelle, M.O. Pekguleryuz, D. Argo, M. Dierks, T. Sparks, T. Waltmate (2001).

[31] D. Wenwen, S. Yangshan, M. Xuegang, X. Feng, Z. Min, W. Dengyun, 356 (2003) 1.

[32] J.A. Hines, R.C. McCune, J.E. Allison, B.R. Powell, L. Ouimet, W.L. Miller, R. Beals, L. Kopka, P.P. Ried, 2006-01-0522 (2006).

[33] H.J. Fuchs, 847992 (1960).

[34] A. Luo, T. Shinoda, 980086 (1998).

[35] K.Y. Sohn, J.W. Jones, J.E. Allison, H.I. Kaplan, J. Hryn, and B. Clow, (2000) 271-278.

[36] A.A. Luo, M.P. Balogh, B.R. Powell, (2002) 33

[37] T. Horie, H. Iwahori, Y. Seno, Y. Awano (2000) 261-269.

[38] Y. Terada, N. Ishimatsu, R. Sota, T. Sato, K. Ohori 419-422 (2003) 459-464.

[39] M. Pekguleryuz, J. Renaud, H. Kaplan, J. Hryn, B. Clow, Warrendale, (2000) 279-284.

[40] A. Suzuki, N.D. Saddock, J.W. Jones, T.M. Pollock, 51 (2004) 1005-1010.

[41] O.D. Sherby, J. Wadsworth, 33 (1989) 169-210.

[42] F.R. Nabarro, 16 (1967) 231-237.

[43] O.D. Sherby, J. Wadsworth, 33(1989) 211-221.

[44] A. Suzuki, N.D. Saddock, J.R. TerBush, B.R. Powell, J.W. Jones, T.M. Pollock, (2007).

[45] D.R. Ni, D.L. Chen, J. Yang, Z.Y. Ma, 56 (2014) 1-8.

[46] D. Amberger, P. Eisenlohr, 60 (2012) 2277–2289

[47] H. Yu, S.N. Chen, W. Yang, Y.L. Zhang, 589 (2014) 479–484

[48] A. Srinivasan, J. Swaminathan, M.K. Gunjan, U.T.S. Pillai, B.C. Pai, 527 (2010) 1395-1403

[49] S. Amira, J. Huot, (2012) 287– 294

[50] J.R. TerBush, A. Suzuki, N.D. Saddock, J.W. Jones, T.M. Pollock, 58 (2008) 914–917

[51] S.M. Zhu, B.L. Mordike, J.F. Nie, 483-484 (2008) 583-586

[52] Q.D. Wang, W.Z. Chen, X.Q. Zeng, Y.Z. Lu, W.J. Ding, Y.P. Zhu, X.P. Xu, 36 (2001) 3035-3040.

[53] L. Han, D.O. Northwood, X. Nie, H. Hu, 512 (2009) 58-66

[54] Y. Zhang, G. Wu, W. Liu, L. Zhang, 595 (2014) 109–117

[55] A.K. Mondal, D. Fechner, S. Kumar, H. Dieringa, P. Maier, K.U. Kainer, 527 (2010) 2289-2296

[56] S. Ji, M. Qian, Z. Fan, 434 (2006) 7–12

[57] J. Kubásek, D. Vojtěch, M. Martínek, 86 (2013) 270–282